

Aus dem Institut für Klinische Neuroimmunologie  
Klinikum der Ludwig-Maximilians-Universität München  
Direktion: Prof. Dr. med. Martin Kerschensteiner

**Contribution of excitatory and inhibitory tract  
components of the reticulospinal tract to  
general locomotion**

Dissertation  
zum Erwerb des Doktorgrades der Medizin  
an der Medizinischen Fakultät der  
Ludwig-Maximilians-Universität zu München

vorgelegt  
von Benjamin Robert Pankratz  
aus Göttingen

2021

Mit Genehmigung der Medizinischen Fakultät  
der Universität München

Berichterstatter: PD Dr. Florence Bareyre

Mitberichterstatter: Prof. Dr. Adrian Danek  
Prof. Dr. Doreen Huppert

Dekan: Prof. Dr. med. dent. Reinhard Hickel

Tag der mündlichen Prüfung: 29.07.2021

---

## Table of Contents

<b>Table of Contents .....</b>	<b>I</b>
<b>List of Figures.....</b>	<b>III</b>
<b>List of Tables .....</b>	<b>IV</b>
<b>List of Abbreviations .....</b>	<b>V</b>
<b>Zusammenfassung .....</b>	<b>VI</b>
<b>Summary.....</b>	<b>VII</b>
<b>1 Introduction .....</b>	<b>1</b>
1.1 Spinal cord injury .....	1
1.1.1 Definition.....	1
1.1.2 Epidemiology .....	1
1.1.3 Clinical course .....	3
1.1.4 Diagnosis and management.....	4
1.1.5 Treatment options.....	5
1.1.6 Pathology.....	7
1.2 Axonal reorganization.....	8
1.2.1 Axonal reorganization in SCI.....	8
1.2.2 Motor cortex .....	9
1.2.3 Corticospinal tract .....	9
1.2.4 Extrapyramidal tracts and brainstem .....	12
1.3 The reticulospinal tract .....	14
1.3.1 Anatomy and function .....	14
1.3.2 Neural subpopulations of the ReST and the gigantocellular nucleus .....	16
<b>2 Objectives .....</b>	<b>17</b>
<b>3 Material and methods .....</b>	<b>18</b>
3.1 Material list.....	18
3.2 Experimental animals .....	21

---

3.3	Methods .....	22
3.3.1	Pharmacological inactivation of neurons using DREADDs.....	22
3.3.2	Viral vector for DREADD transmission and labeling.....	22
3.3.3	Virus injection .....	23
3.3.4	Tissue processing.....	24
3.3.5	Behavioral tests .....	25
3.3.6	Data analysis.....	29
<b>4</b>	<b>Results.....</b>	<b>31</b>
4.1	Behavioral analysis of mice after silencing of neural subpopulations of the NRG .	31
<b>5</b>	<b>Discussion .....</b>	<b>41</b>
5.1	Summary.....	41
5.2	Potential and limitations of used methods .....	41
5.2.1	DREADD induced silencing of neural subpopulations .....	41
5.2.2	Selection of behavioral tests .....	43
5.3	The NRG's physiologic contribution to general locomotion.....	44
5.4	Future strategies to investigate the ReST's potential for recovery from SCI .....	46
<b>6</b>	<b>References .....</b>	<b>48</b>
<b>7</b>	<b>Acknowledgements .....</b>	<b>55</b>

---

## List of Figures

Figure 1: Global map of tSCI incidences. ....	2
Figure 2: Global distribution of etiology of tSCI. ....	3
Figure 3: Spinal cord tracts and classic lesion patterns. ....	4
Figure 4: Surgical decompression and fusion of the spinal cord after tSCI. ....	6
Figure 5: Schematic detour circuit of the CST in a dorsal hemisection model. ....	10
Figure 6: Anatomy of motoric tracts from the brain to the spinal cord. ....	11
Figure 7: The ipsilateral NRG showed the highest increase in labelled neurons following SCI. ....	13
Figure 8: Different nuclei of the reticulospinal tract in the mouse brainstem. ....	14
Figure 9: Anatomical distribution of the ReST in the spinal cord of the mouse. ....	15
Figure 11: Presynaptic marker distribution of motor tracts in the rat. ....	16
Figure 12: Cre-loxP system. ....	23
Figure 13: Example picture of a virus injection in the NRG. ....	24
Figure 14: Exemplary analysis of stepping patterns in the CatWalk software. ....	27
Figure 15: Exemplary calculation of Couplings. ....	28
Figure 16: Schematic camera view of a mouse on the CatWalk. ....	29
Figure 17: Viral injection sites. ....	32
Figure 18: Experimental setup. ....	32
Figure 19: Fixed and accelerated rotarod results. ....	33
Figure 20: Regular and irregular ladder rung results. ....	34
Figure 21: CatWalk principal component analysis results. ....	36
Figure 22: Factor loadings of PC1 of CTRL. ....	37
Figure 23: Regularity index results. ....	37
Figure 24: Couplings results. ....	40
Figure 25: Base of support results. ....	40

---

## List of Tables

Table 1: List of normal step sequence patterns recognized by the software. ....	27
Table 2: Definition of the different groups of the experiment. ....	31

---

## List of Abbreviations

BOS	base of support
cloz	clozapine
CST	corticospinal tract
CT	computer tomography
DGN	Deutsche Gesellschaft für Neurologie
dpi	days post virus injection
DREADD	Designer Receptors Exclusively Activated by Designer Drugs
FL	forelimbs
GOI	gene of interest
HL	hindlimbs
i.p.	intraperitoneal
LPGi	lateral paragigantocellular nucleus
LPN	long propriospinal neurons
mil	million
MRI	magnetic resonance imaging
NRG	gigantocellular nucleus
PCA	principal component analysis
ReST	reticulospinal tract
RI	regularity index
RT	rubrospinal tract
SCI	spinal cord injury
SEM	standard error of the mean
tSCI	traumatic spinal cord injury
VGAT	vesicular GABA transporter
VGLUT1/2	vesicular glutamate transporter 1/2
VST	vestibulospinal tract

---

## Zusammenfassung

Die traumatische Rückenmarksverletzung ist eine verheerende Krankheit des Rückenmarks, die nach plötzlichem, primärem Einsetzen der Verletzung zu einer sekundären Verletzungskaskade führt, welche das Rückenmark weiter schädigt und endogene Erholung limitiert. Einer der zahlreichen therapeutischen Strategien zielt auf diese regenerativen Kapazitäten ab, indem sie die axonale Reorganisation von motorischen Trakten erleichtert. Da sich die bisherige Forschung hauptsächlich auf den *Tractus corticospinalis* richtete, ist deutlich weniger über die regenerativen Kapazitäten von extrapyramidalen Trakten bekannt. Aufgrund dessen, dass der *Tractus reticulospinalis* vermutlich an allgemeiner Fortbewegung in physiologischen Zuständen beteiligt ist, wird angenommen, dass er von großer Bedeutung in Hinblick auf das Wiedererlangen der Gehfähigkeit nach Rückenmarksverletzung beim Menschen ist. Deswegen untersuchte ich den physiologischen Beitrag von zwei neuronalen Subpopulationen des *Nucleus gigantocellularis* (NRG), einer der Nuclei des *Tractus reticulospinalis*, zur allgemeinen Fortbewegung in Mäusen. Ich verwendete einen viralen Vektor, um cre-abhängige Designer Receptors Exclusively Activated by Designer Drugs (DREADDs) in den NRG von zwei unterschiedlichen, transgenen Mauslinien zu injizieren, wodurch entweder exzitatorische oder inhibitorische Neurone abgeschaltet wurden. Nach Erreichen einer ausreichenden Virusausbreitung testete ich das Verhalten der Mäuse vor und nach Abschalten der Zielneurone mit den Verhaltenstests rotarod, ladder rung und CatWalk. Meine Ergebnisse zeigen übereinstimmend keine Verhaltensveränderungen der Mäuse nach Abschalten von neuronalen Subpopulationen des NRG im Vergleich zu Kontrollen. Im Einklang mit nachfolgender Forschung anderer Forschungsgruppen scheinen die physiologischen Funktionen des NRG in Hinblick auf allgemeine Fortbewegung hauptsächlich von supportiver Natur zu sein, während essenzielle Beiträge von anderen Nuclei des *Tractus reticulospinalis* stammen, vor allem von dem *Nucleus paragigantocellularis lateralis*. Da regenerative Kapazitäten nach Rückenmarksverletzung jedoch für mehrere Nuclei einschließlich des NRG beschrieben wurden, wird weitere Forschung nötig sein, die die Beziehungen zwischen ihren physiologischen und regenerativen Funktionen aufdeckt, um Angriffspunkte zur Steigerung der axonalen Reorganisation zu formulieren.

---

## Summary

Traumatic spinal cord injury is a devastating disease of the spinal cord, that after its primary sudden onset, leads to a secondary injury cascade, which further damages the spinal cord and limits endogenous recovery. One of the many therapeutic strategies targeting the regenerative capacities is to facilitate axonal reorganization of motoric tracts. While research has focused mainly on the corticospinal tract, much less is known about the regenerative capacities of extrapyramidal tracts. As the reticulospinal tract is supposedly involved in general locomotion in physiologic states, it is theorized to be of major importance regarding the recovery of the ability to walk after spinal cord injury in humans. Therefore, I investigated the physiologic contribution of two neural subpopulations of the gigantocellular nucleus (NRG), one of the nuclei of the reticulospinal tract, to general locomotion in mice. Using a viral vector, I injected cre-dependent Designer Receptors Exclusively Activated by Designer Drugs (DREADDs) into the NRG of two different transgenic mouse lines, in order to silence either excitatory or inhibitory neurons. After sufficient viral spread, I tested mice behaviorally before and after silencing target neurons on the rotarod, ladder rung and CatWalk. My results consistently show no behavioral alterations following the silencing of neural subpopulations of the NRG in comparison to controls. In accordance with subsequent research from other labs, the physiologic functions of the NRG regarding general locomotion seem to predominantly be of supportive nature, while essential contributions derive from other nuclei of the reticulospinal tract, especially from the lateral paragigantocellular nucleus. However, as regenerative capabilities following spinal cord injury have been described for multiple nuclei including the NRG, further research is needed to untangle the relationships of their physiologic and regenerative functions in order to formulate targets for improved axonal reorganization.

# **1 Introduction**

## **1.1 Spinal cord injury**

The sudden onset and severity of spinal cord injury changes a person's life in every aspect. The physical, psychological, social and vocational integrity of the patient are often compromised for a lifetime, which is reflected by lifelong increased mortality rates and decreased quality of life (Dijkers, 1997; Ahuja et al., 2017). Additionally, the total financial burden of a patient with spinal cord injury (SCI) for society ranges from about 1.2 mil to 5 mil US\$ (National Spinal Cord Injury Statistical Center, 2012).

The dogma of the inert, adult central nervous system (CNS), incapable of regeneration, has long been dismantled, shedding hope for treatment for this devastating condition. Indeed, preclinical research of the last decades has produced an intriguing arsenal of potential treatment options, that are now being tested in clinical trials (Kim et al., 2017).

### **1.1.1 Definition**

SCI is defined as damage to the spinal cord, which consists of grey matter and white matter. It usually is divided etiologically into nontraumatic and traumatic spinal cord injury (tSCI). After the primary injury, a complex secondary injury cascade follows, which provides a frame for interventional, neuroprotective treatment. Intrinsic regenerative and compensatory strategies are potent in the spinal cord, however limited by inhibitory mechanisms of the disease, often leaving patients with tetra- or paraplegia and a range of neurologic symptoms.

### **1.1.2 Epidemiology**

Global epidemiologic data on traumatic SCI is difficult to evaluate, as most studies were conducted on a regional or national level showing great variation between developed and undeveloped countries (Singh et al., 2014). Concerning Germany, sparsity and methodical flaws only allow for estimates based on retrospectively collected data from specialized treatment facilities, that can be translated to an incidence of about 10.7/mil (Exner et al., 2004).

While comparable numbers persist throughout Europe, the incidence in the U.S. with 40-50/mil is much higher (Figure 1). Reliable data on the prevalence of tSCI is not available for Germany. In the U.S. though, calculated prevalence ranges from 525-906/mil, depending on the data and methods used (Singh et al., 2014).

Vehicular accidents are the leading cause of traumatic SCI (38.1%), followed by falls (31.0%), violence (13.5%) and sports (8.9%; Figure 2; Chen et al., 2016). There is a first age peak in the group of 15-30 years old people with a male to female ratio of about 4:1. A trend towards a second age peak in individuals over 50 years of age due to falls can be observed in more recent studies (Ahuja et al., 2017).

Making up almost two thirds of all tSCI, lesions at the cervical level remain the most common, explaining the high portion of tetraplegia. Thoracic and lumbar lesions significantly trail behind (Chet et al., 2016).

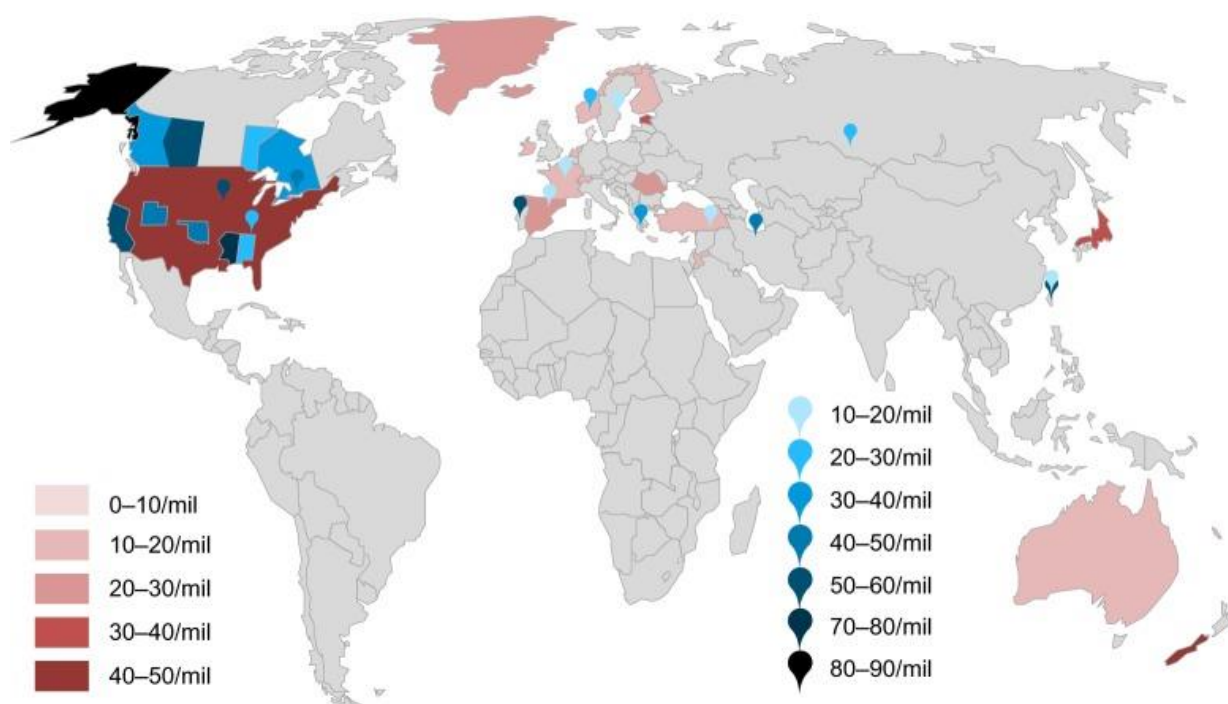


**Figure 1: Global map of tSCI incidences.** Red color illustrates national incidences of tSCI. Blue color illustrates regional incidences within a nation. mil: million. Adapted from Singh et al., 2014.

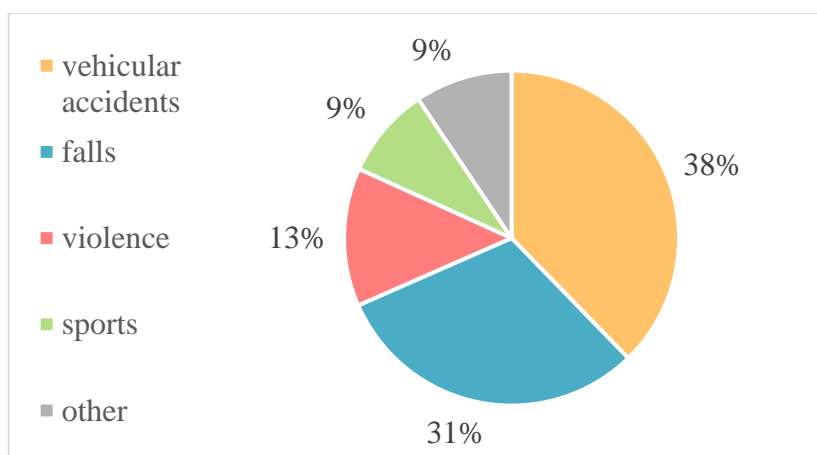


**Figure 2: Global distribution of etiology of tSCI.** Vehicular accidents and falls make up for more than two thirds of all etiologies. After Singh et al., 2014.

### 1.1.3 Clinical course

The clinical features of tSCI vary greatly depending on the level and pattern of the lesion within the spinal cord (Figure 3). In general, sensory-motor deficits below the level of the lesion, respiratory failure, intestinal and bladder dysfunction, sympathetic dysfunction, spasticity and neuropathic pain form the range of frequent symptoms.

Cervical lesions include motoric outputs of the upper extremities, which leads to tetraplegia, while lower lesions cause paraplegia. Respiratory failure to different extents might occur if the diaphragm or other respiratory muscles are involved. Decreased peripheral vascular tone, due to sympathetic dysfunction, and decreased muscular tone with restricted venous return, due to plegia, can result in hypotension. A lesion above T6 might additionally affect splanchnic nerves and sympathetic cardiac input, which induces bradycardia (Ahuja et al., 2017). The maximal variant of this mechanism, neurogenic shock, can be seen in about 20% of patients with cervical SCI (Guly et al., 2008).

#### Spinal shock

Spinal shock is the clinical manifestation of temporary flaccid paralysis and depression of deep tendon reflexes, that sets in directly after the incident. It is not uniformly defined, but recent advances think of it as a four-phase development, that takes weeks to months to turn into a state of hyperreflexia and spasticity (Dittuno et al., 2004).

#### Chronic symptoms

Despite successful effects of rehabilitation, in most cases disabling sensory-motor and autonomic deficits persist. Additionally, when reaching chronicity, treatment refractory

neuropathic pain can be seen in 40% of tSCI patients 1.2 years after onset, often together with spasticity, that reaches prevalences up to 75% 1.0 years after onset (Adam and Hicks, 2005; Cardenas and Felix, 2009).

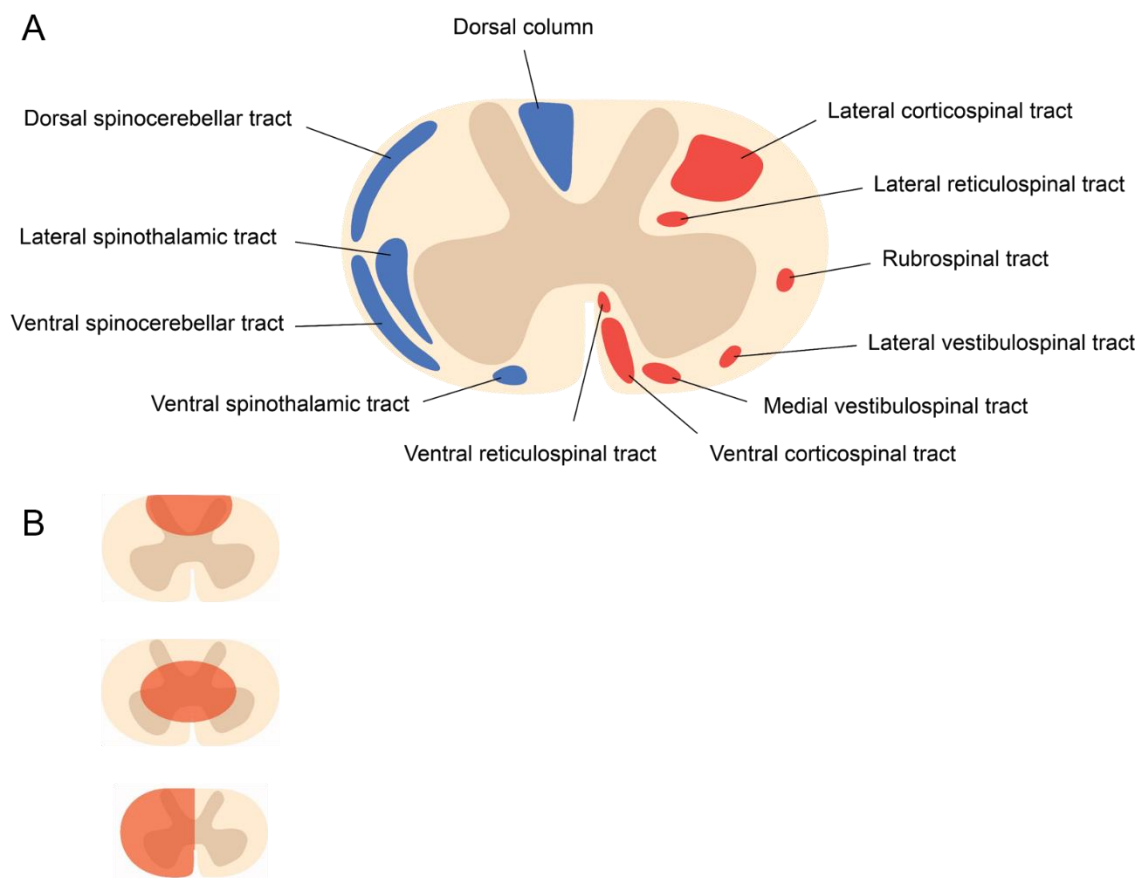


**Figure 3: Spinal cord tracts and classic lesion patterns.** **A** | Schematic spinal cord section showing the anatomy of spinal cord tracts in humans. Blue: sensory tracts. Red: motor tracts. **B** | Examples of the diversity of potential injury patterns and clinical manifestations. Upper: Anterior spinal artery syndrome. Middle: Central cord syndrome. Lower: Brown-Sequard syndrome. Red area: lesioned area.

#### 1.1.4 Diagnosis and management

Due to its etiological nature, tSCI requires in-field medical care consisting of securing airways, breathing, circulation and spine immobilization using cervical collars and spine or vacuum boards (Ahuja and Martin, 2016). Upon arrival in the hospital, patients with suspected tSCI or polytrauma usually undergo specific diagnostic and therapeutic algorithms, with the Advanced Trauma Life Support being one of the typical systems used in Germany. Within the first steps in these algorithms should be a neurological examination, preferably on base of the International Standards for Neurological

---

Classification of Spinal Cord Injury (Kirshblum et al., 2011), which is a standardized grading system for sensory-motor function in patients with SCI, that was shown to possess high inter-rater reliability and reproducibility (Marino et al., 2018). Clinical examination is the most important functional parameter and early assessments can serve as baselines throughout the course of the disease (Ahuja et al., 2017).

Imaging also plays an essential role in the diagnosis of SCI. German polytrauma guidelines recommend the full-body CT scan as the initial imaging modality of choice, screening for bony spine injuries (Lendemans and Ruchholtz, 2012). These injuries are classified with the AOSpine classification system and can give hints about spine stability (Vaccaro et al., 2013, 2016). Concerning the evaluation of soft tissue including the spinal cord, the MRI remains the superior imaging option and is correlated to the severity of SCIs as well as to prognostic outcomes (Lammertse et al., 2007).

### **1.1.5 Treatment options**

#### **Surgical intervention**

Surgical intervention for treatment of SCI includes open reduction, decompression of the spinal cord and subsequent mechanical stabilization of dislocated structures utilizing a variety of different surgical techniques aiming for fusion and fixation (Figure 4). However, questions of efficacy and timing of this intervention still remain unclear (Fehlings et al., 2017).

A meta-analysis of preclinical studies showed positive effects of surgical decompression in animal models in regard of behavioral outcomes. The negative influence of the amount of pressure and the duration of the compression on outcomes hint at early time points being favorable (Batchelor et al., 2013).

Unfortunately, translation to human patients has been conducted inconsistently, as studies have used different thresholds for the time of the intervention, which has led to poor evidence (Fehlings et al., 2006). Though, more recent studies suggest surgical intervention within 24 h of disease onset, since this timeframe holds advantages in terms of neurological outcome and complication rate (Fehlings et al., 2012).

The German guidelines of the Deutsche Gesellschaft für Neurologie (DGN) merely recommend „swift surgical decompression and stabilization“, leaving optimal timing open to interpretation („Leitlinien für Diagnostik und Therapie in der Neurologie“, 2012).

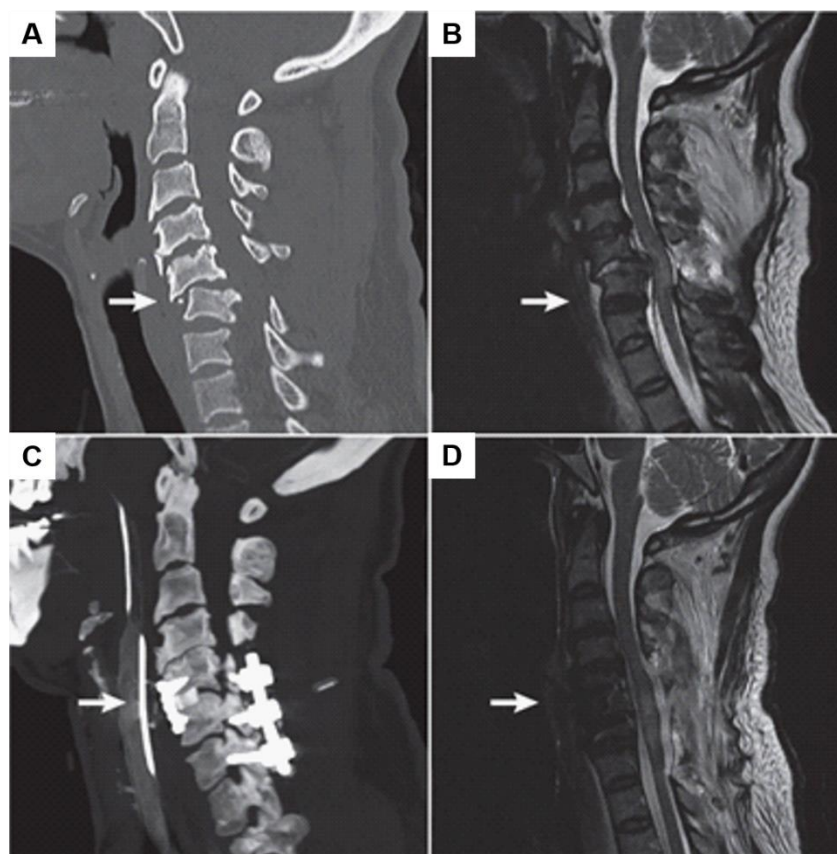


**Figure 4: Surgical decompression and fusion of the spinal cord after tSCI.** **A** | CT scan of the cervical spine shows a C5/C6 fracture with dislocation. **B** | MRI scan reveals compression of the spinal cord. **C** | Postoperative CT scan after surgical decompression and fusion of C5/C6/C7. **D** | MRI scan demonstrates successful decompression of the spinal cord. Arrows indicate the cervical level C5/C6. Adapted from Ahuja et al., 2017.

### **Methylprednisolone**

The debate about the use of methylprednisolone in the treatment of SCI has been ongoing since the discovery of its promising effects in preclinical experiments, in which it showed anti-inflammatory effects and beneficial modulations of several pathophysiological mechanisms (Hall and Braughler, 1982, 1984). However, clinical trials that followed, including the NASCIS studies (Bracken and Holford, 1993; Bracken et al., 1997), were not able to generate conclusive data. Positive effects could not consistently be reproduced,

---

while adverse effects are indisputable (Silva et al., 2014). Furthermore, the use of subgroup analysis in order to show effect, has been criticized (Fehlings et al., 2017).

The debate has led to changing recommendations over the years. Most guidelines do not longer recommend methylprednisolone as a standard therapy. Guidelines of the AOSpine, an international, renowned organisation of spine surgeons and researchers, suggest the application of a 24 h infusion of methylprednisolone as a possible treatment option (Fehlings et al., 2017).

The DGN makes the same suggestion for patients with isolated tSCI and does not recommend it for polytrauma patients („Leitlinien für Diagnostik und Therapie in der Neurologie“, 2012). Lastly, the decision should always be patient-dependent and is up to the attending physician.

### **1.1.6 Pathology**

In tSCI, damage to the spinal cord occurs in two phases. Primary injury consists of immediate mechanical damage via laceration, distraction, transection or compression, which often persists because of dislocation (Dumont et al., 2001). Secondary injury, mediated by a cascade of biochemical alterations, starts minutes after the incident and involves vascular changes, electrolyte changes, lipid peroxidation, excitotoxicity, apoptosis, and inflammation (Sekhon and Fehlings, 2001). It continues over months and gradually evolves into a chronic state. While damage through primary injury cannot be prevented in most cases, secondary injury offers a convenient time frame for intervention and its pathophysiological mechanisms have been intensely studied over the last decades.

Vascular changes include hemorrhage, vasospasms, thrombosis, and disruption of autoregulation, all leading to ischemia and necrosis of neural tissue within hours of onset (Silva et al., 2014). Additionally, a large quantity of free radicals, mostly oxygen and nitrogen species, is produced causing lipid peroxidation, a process that damages and lyses membranes (Oyinbo, 2011). Changes in electrolyte concentrations concern sodium, potassium and calcium, with the latter being the main mediator of apoptosis. Calcium induces upregulation of apoptosis-related proteases, caspases and calpain, which break down the cytoskeleton of the cell resulting in apoptosis (Ray et al., 2003). Furthermore, it has been shown, that dying neurons and glia release high amounts of glutamate to their

---

environment. The neurotransmitter binds mostly to NMDA-receptors of intact cells and can induce neurotoxicity through excessive excitation (Liu et al., 2010).

## **Inflammation**

Disturbance of the blood barrier following primary injury enables infiltration of leucocytes including macrophages, T-cells and neutrophils. They release cytokines attracting further immune cells and induce inflammation (Bareyre and Schwab, 2003). Inflammation and its role in SCI is still nebulous and double edged. On the one hand, it has been shown, that inflammatory mechanisms can amplify damage to the spinal cord through release of biochemical molecules and enzymes as well as through autoimmunity of lymphocytes. On the other hand, leucocytes have the potential to mediate neuroprotection and regeneration via trophic support, synthesis of neurotrophic factors and axon guidance (Donnelly and Popovich, 2008). The relation of these conflictive observations remains obscure. However, it is theorized, that timing plays an important role, with early inflammation predominantly causing damage (Klusman and Schwab, 1997).

## **1.2 Axonal reorganization**

Battling with the pathophysiologic injury cascade, known intrinsic and extrinsic possibilities for regeneration or compensation are now diverse and seem promising. Therapeutic strategies can roughly be divided into the categories of neuroprotection and neuroregeneration. Neuroprotection aims at attenuating the effects of the secondary injury cascade, as it is the case in surgical interventions or in the application of methylprednisolone. In contrast to that, neuroregeneration aims at promoting intrinsic mechanisms of regeneration. Main approaches at the moment include transplantation of stem cells, disinhibition of key pathways preventing intrinsic, regenerative capacity and promotion of axonal reorganization of motoric tracts (McDonald et al., 1999; Liebscher et al., 2005; van den Brand et al., 2012). As this thesis focuses on motoric tracts and systems, the following will elaborate on axonal reorganization in SCI.

### **1.2.1 Axonal reorganization in SCI**

The dogma of an inert CNS lacking regenerative capacity has been abandoned a long time ago. Following SCI, a variety of adaptations on different levels in the CNS, including the

---

cortex, brainstem and spinal cord, occur to different extents depending on the injury pattern. True regeneration, in the sense of a *restitutio ad integrum*, that would require neurogenesis or a reconnection of damaged axons as before, has failed to be observed in a relevant proportion in the spinal cord. In fact, the CNS mainly relies on axonal reorganization to promote functional recovery after SCI (Silva et al., 2014).

### **1.2.2 Motor cortex**

The motor cortex is arranged in a topographic system and is crucial for voluntary movement. After SCI, cortical representation of deafferented areas below the lesion is partly or fully abolished and cortical reorganization takes place in areas projecting both rostrally and caudally to the lesion (Brown and Martinez, 2019). Conceptually, it can be differentiated between two types of reorganization, depending on which hemisphere of the cortex is involved.

Firstly, motor cortex areas that lose their output following SCI tend to be taken over by intact ipsilateral motor cortex areas, which then mediate some regained functionality regarding locomotion, probably by using different movement patterns than before (Bareyre, 2004; Manohar et al., 2017).

Secondly, in unilateral lesions, the ipsilesional and therefore mostly unaffected motor cortex undergoes plasticity as well, adopting representation of the abolished area of the opposite hemisphere. As this reorganization carries function, it appears to support recovery (Brown and Martinez, 2018).

### **1.2.3 Corticospinal tract**

The corticospinal tract (CST, Figure 6) has been the most extensively studied model for intraspinal reorganization. In mammals, it is highly conserved as the main motoric tract for voluntary movement (Brown and Martinez, 2019). After SCI, injured as well as spared CST fibers are able to sprout and form new synapses (O'Shea et al., 2017). Spared CST fibers, e.g. fibers of the ventral CST in a dorsal hemisection model, can sprout, traverse the spinal cord and build synapses on deafferented motor neurons, that promote function (Weidner et al., 2001; Bareyre et al., 2004; Bareyre et al., 2005).

The sprouting of injured axons rostrally and caudally to a lesion enables them to contact long propriospinal neurons (LPN), which are intraspinal interneurons reaching from the

cervical cord to the lumbar cord. In a two-phase process consisting of unguided sprouting and selection of beneficial synapses, LPN can be contacted on both sides of the lesion, so that injured fibers are able to target their initial outputs (Figure 5; Bareyre et al., 2004). The formation of this detour circuit bypassing the lesion site was repeatedly shown to support powerful recovery of motoric functions (Bareyre et al., 2004; Courtine et al., 2008).

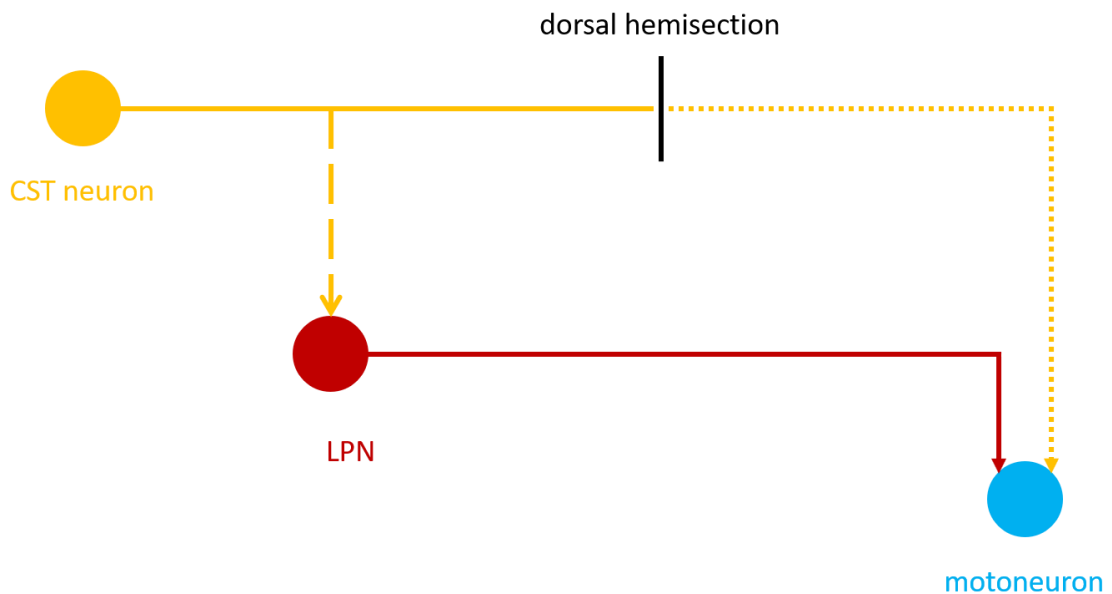


**Figure 5: Schematic detour circuit of the CST in a dorsal hemisection model.** After dorsal hemisection, CST neurons are able to form a detour circuit by sprouting and contacting long propriospinal neurons. Dotted line represents deafferented axons. Dashed line represents newly sprouted collaterals. CST: corticospinal tract. LPN: long propriospinal neuron. Adapted from Jacobi et al., 2015.

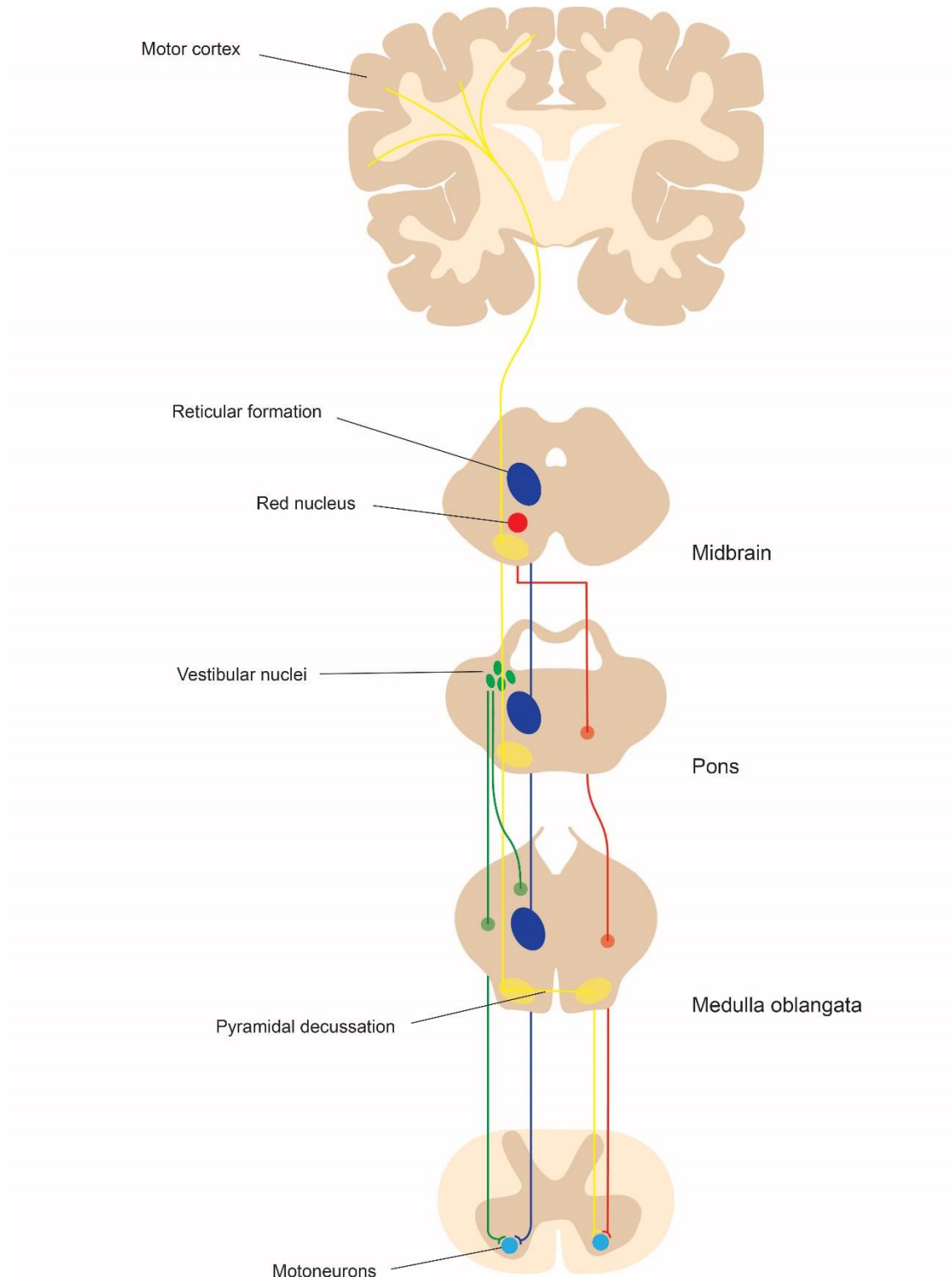


**Figure 6: Anatomy of motoric tracts from the brain to the spinal cord.** Origin and course of the corticospinal tract and extrapyramidal tracts. Yellow: corticospinal tract. Blue: reticulospinal tract. Red: rubrospinal tract. Green: vestibulospinal tract. For clarity, bilateral projections are not shown; presented is the major projection of every tract.

---

#### 1.2.4 Extrapyramidal tracts and brainstem

In rodents, the rubrospinal tract (RT, Figure 6) contributes to skilled movements and thus, shares similarities in function with the CST (Whishaw et al., 1998). In humans, however, it is developed to much lesser extent and presumably holds much lesser impact on movement (Vadhan and Das, 2019). The vestibular tract (VT) and the reticulospinal tract (ReST, Figure 6) conceptually and conversely to the CST and RT hold function to involuntary movements and therefore to general locomotion. The VT is believed to mediate posture, balance and head stability, which are requirements for effective locomotion (Markham, 1987; McCall et al., 2017). The ReST is supposed to be directly involved in the generation and functionality of propulsive locomotion (Noga et al., 2003).

Because the latter translates to the general ability of walking in humans, which is a major therapeutic goal in SCI, more interest has shifted to the investigation of the ReST over the last years. Indeed, several studies were able to demonstrate a high capacity of anatomical plasticity of the ReST. After SCI, fibers of the ReST are able to sprout caudal as well as rostral to a lesion, forming a detour circuit similar to the one involving the CST, by making contact to midline crossing propriospinal neurons. This ReST reorganization also held considerable functional recovery (Ballerman and Fouad, 2006; Filli et al., 2014). Furthermore, using a hemilesion model in rats, one study addressed the differences in anatomical plasticity of extrapyramidal tracts. It not only qualified the ReST as the most plastic tract among the extrapyramidal tracts, but also showed, that its intraspinal plasticity is paralleled by brainstem reorganization (Zörner et al., 2014). Through retrograde tracing, the nucleus mostly involved in this reorganization was determined to be the gigantocellular nucleus (NRG) of the reticular formation in the brainstem (Figure 7; Ballerman and Fouad, 2006; Filli et al., 2014).

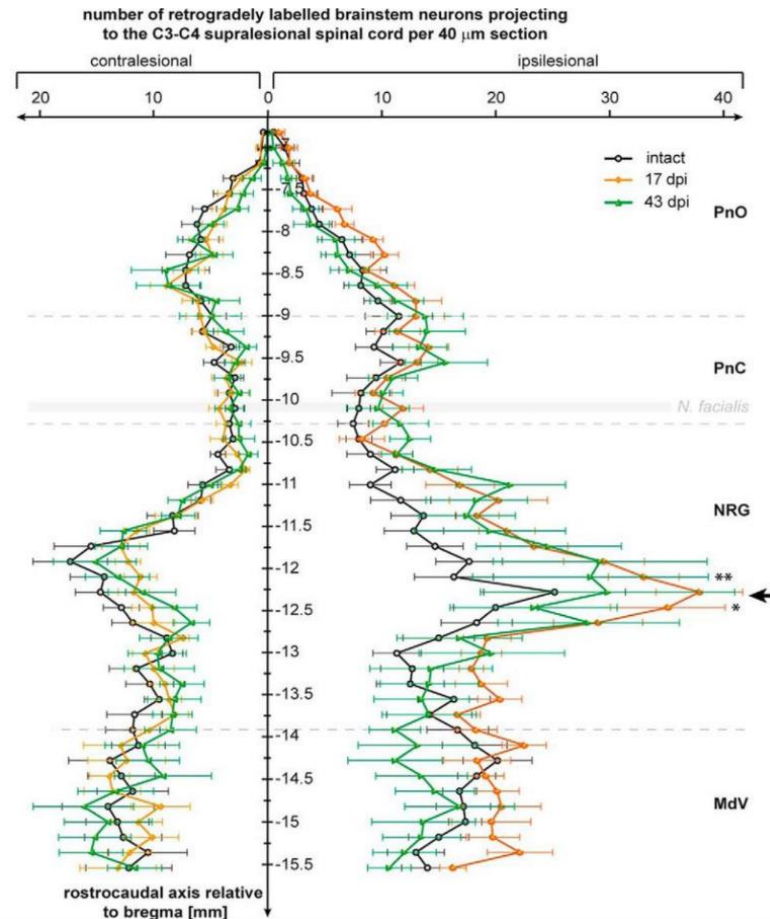


**Figure 7: The ipsilateral NRG showed the highest increase in labelled neurons following SCI.** In a unilateral hemisection model in the rat, the number of neurons of different origins in the brainstem, retrogradely traced by fibers from the cervical spinal cord C3/4, were quantified before and after SCI. The NRG had the highest increase in labelled neurons, which hints at its capacity of plasticity. \* $P < 0.05$ . \*\* $P < 0.01$ . Adapted from Filli et al., 2014.

## 1.3 The reticulospinal tract

### 1.3.1 Anatomy and function

The ReST originates from a dispersed set of nuclei, namely the gigantocellular nucleus, lateral paragigantocellular nucleus, dorsal paragigantocellular nucleus, alpha gigantocellular nucleus and ventral gigantocellular nucleus (Figure 8) in the medial pontomedullary reticular formation of the brainstem (Wang, 2009).

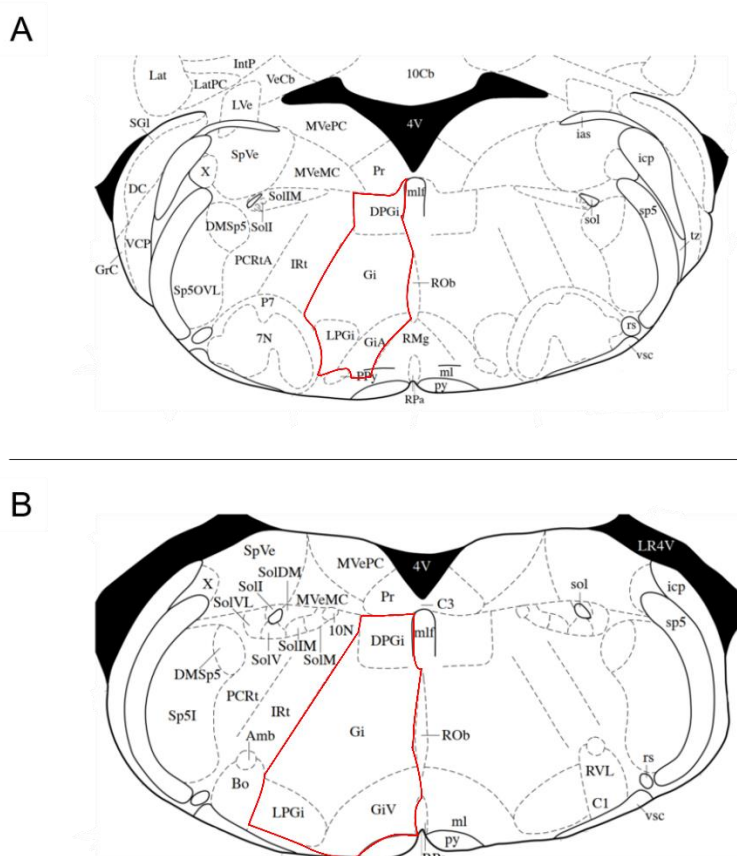


**Figure 8: Different nuclei of the reticulospinal tract in the mouse brainstem. A |** Coronal section -6,24mm from bregma. **B |** Coronal section -6,64mm from bregma. Red markings: nuclei of the ReST. Gi: gigantocellular nucleus. LPGi: lateral paragigantocellular nucleus. GiA: alpha gigantocellular nucleus. GiV: ventral gigantocellular nucleus. DPGi: dorsal paragigantocellular nucleus. Adapted from Paxinos and Franklin, 2001.

Its axons travel bilaterally, with most of the fibers running diffusely on the ipsilateral side in the ventral and lateral parts of the white matter of the spinal cord (Figure 9; Nathan et al., 1996; Ballerman and Fouad, 2006). On the one hand, they project directly onto motor neurons of the spinal cord, which correlates to the ReST's contribution to skilled forelimb movements (Soteropoulos et al., 2012; Honeycutt et al., 2013). On the other hand, the ReST projects onto and modulates central pattern generators of the spinal cord, that generate distinct muscle activation patterns for general locomotion like walking (Jordan, 1998). Hereby, the ReST acts as a relay and receives its input from upper motoric command centers in the brainstem, namely the mesopontine and diencephalic locomotor regions (MLR, DLR; Noga et al., 2003). These regions are highly conserved among vertebrates and are able to produce walking movements on their own in decerebrated lower mammals, if stimulated (Grillner et al., 2017).

These findings imply a primary role of the ReST and the NRG in general locomotion. However, not much is known about the concrete, relative contribution and importance to locomotor functions of the ReST in neither physiological states nor following spinal cord lesions. Besides, the different nuclei and neural subpopulations might have substantial differences in their functions and contributions. As lesion studies of the ReST repeatedly highlighted the role of the NRG in anatomical plasticity, as stated above, it appears to be the most promising target in the search for recovery mechanisms regarding axonal reorganization in extrapyramidal tracts.

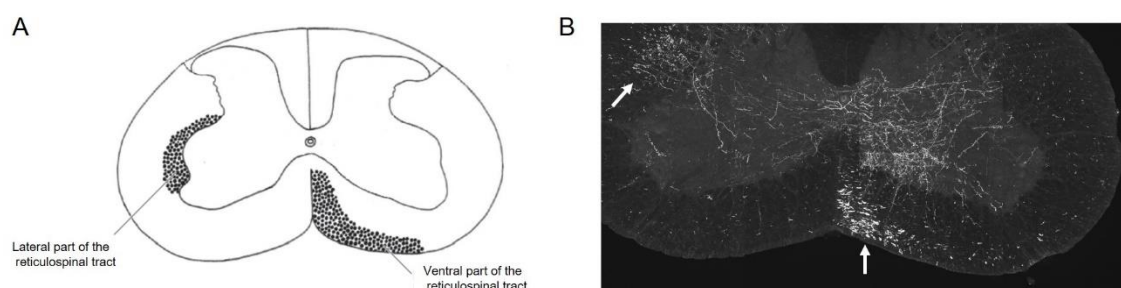


**Figure 9: Anatomical distribution of the ReST in the spinal cord of the mouse.** **A** | Lateral and ventral part of the ReST in the spinal cord. **B** | Anterograde tracing of fibers of the NRG of the ReST. Coronal section at C1 of the spinal cord. Left arrow: lateral part of the ReST. Right arrow: ventral part of the ReST.

### 1.3.2 Neural subpopulations of the ReST and the gigantocellular nucleus

Using colocalization of anterograde fluorescent and presynaptic markers, two studies examined the composition of the ReST and the NRG. The first study showed, that the ReST, in contrast to other motoric tracts, is composed of different neural subpopulations with different neurotransmitters mediating excitation as well as inhibition (Figure 11: Du Beau et al., 2012). The same approach focusing solely on the NRG provided similar results with minor differences (Figure 11). It confirmed the predominant portion of glutamatergic efferences (20.6% VGLUT1 positive, 71.6% VGLUT2 positive) with a smaller fraction of gabaergic efferences (7.8% VGAT positive; Filli et al., 2014). While the excitatory role for movements of VGLUT positive fibers of the ReST was exhibited, the specific functions of the different subpopulations of the NRG and its contributions to recovery after SCI remain unknown (Hägglung et al., 2010).

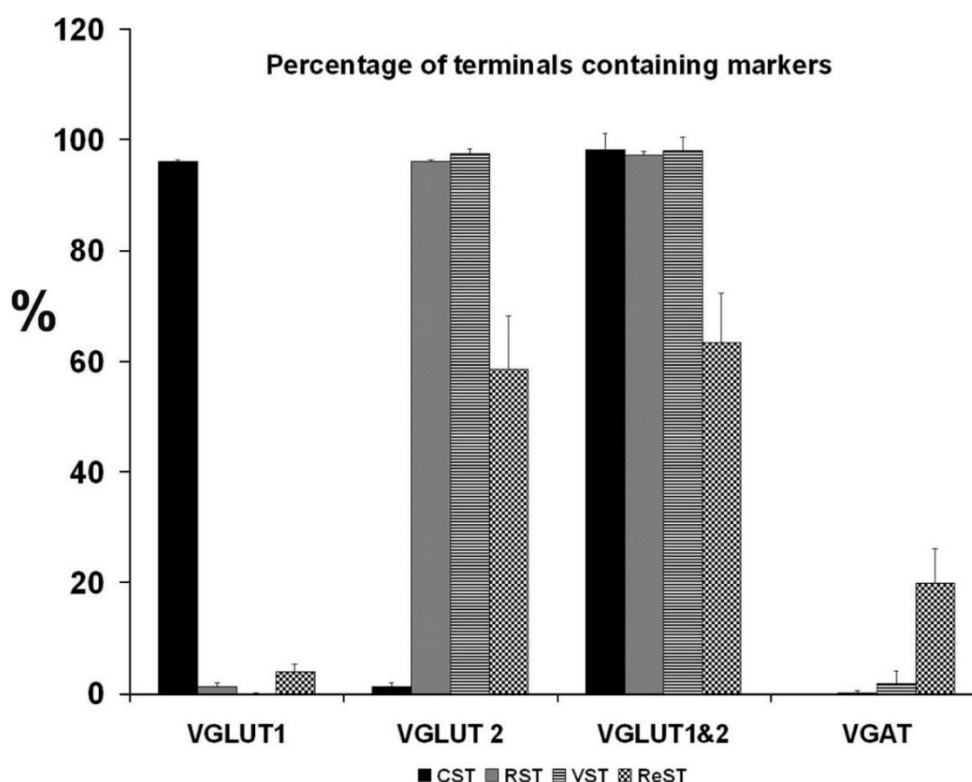


**Figure 11: Presynaptic marker distribution of motor tracts in the rat.** Distribution of stained fibers of different tracts with immunoreactive markers for presynaptic transporters. The ReST's proportion of VGAT positive fibers is substantially higher than those of the other tracts, which are mainly VGLUT positive. VGLUT1: vesicular glutamate transporter 1. VGLUT2: vesicular glutamate transporter 2. VGAT: vesicular GABA transporter. Adapted from Du Beau et al., 2012.

---

## 2 Objectives

The reticulospinal tract mediates general locomotion and is capable of both neuroanatomical plasticity and functional recovery following SCI. Research has only begun to dissect the functional contributions of different nuclei and neural subpopulations of the ReST. Recently, it focused on the NRG as a potential candidate crucially involved in recovery after SCI. However, to date, not much is known about its physiologic functions. This study, therefore, aims to characterize the functional contribution of NRG nuclei to general locomotion and evaluates the role of the NRG as a potential target of interest in SCI research. In detail, this work engages in the following questions:

- What is the NRG's physiologic contribution to general locomotion?
- What is the contribution of excitatory and inhibitory subpopulations of NRG upper neurons to general locomotion?
- Should future SCI research on the ReST focus on the NRG?

### 3 Material and methods

#### 3.1 Material list

Reagent	Retailer
Agarose	Sigma-Aldrich® Chemie GmbH, 82024 Taufkirchen, Germany
Bepanthen Augen- und Nasensalbe 5 g (eye ointment)	Bayer Vital GmbH, Leverkusen, Germany
Clozapine	Sigma-Aldrich® Chemie GmbH, 82024 Taufkirchen, Germany
Ethanol 70%	CLN GmbH, 85416 Niederhummel, Germany
Forene (Isoflurane)	Abbott AG, Baar, Switzerland
Hydrogen Peroxide Solution (H <sub>2</sub> O <sub>2</sub> )	Sigma-Aldrich® Chemie GmbH, 82024, Taufkirchen, Germany
Ringerlösung Fresenius KabiPac (Ringer's solution)	Fresenius KaBI Dtl., Bad Homburg, Germany
Phosphate Buffer (PB) 0,2 M	27,598 g NaH <sub>2</sub> PO <sub>4</sub> ·H <sub>2</sub> O; 35,598 g Na <sub>2</sub> HPO <sub>4</sub> ·2 H <sub>2</sub> O; dH <sub>2</sub> O ad 1 l
Paraformaldehyde 4%	8% PFA (Sigma-Aldrich) in dH <sub>2</sub> O, heated up to 55 °C and stirred additional 10 min, filtrated and mixed in a 1:1 ratio with 0,2 M PB (Phosphate buffer), pH adjusted to 7,2-7,8
Phosphate Buffered Saline (PBS), 10x	03,23 mg Na <sub>2</sub> HPO <sub>4</sub> ·H <sub>2</sub> O; 26,52g Na <sub>2</sub> HPO <sub>4</sub> ·2H <sub>2</sub> O; 40g NaCl; H <sub>2</sub> O bidest. added to 1 l. Prepared in house.

---

Sucrose	Sigma-Aldrich® Chemie GmbH, 82024, Taufkirchen, Germany
Tissue Tek optimal cutting temperature (O.C.T.)	Sakura Finetek Europe B.V., Alphen aan den Rijn, The Netherlands
Triton X-100	Sigma-Aldrich® Chemie GmbH, 82024 , Taufkirchen, Germany
Vectashield Mounting Medium, Fluorescence H-1000 Vectashield Mounting Medium, Fluorescence H-1000	Vector Labs, Burlingame, CA 94010, USA

<b>Virus</b>	<b>Retailer</b>
AAV-hSyn-DIO-hM4D(Gi)-mCherry	Addgene, Watertown, MA 02472, USA

<b>Surgical tools and materials</b>	<b>Retailer</b>
50 ml centrifuge tubes	Greiner Bio-One GmbH, Frickenhausen, Germany
BD Plastipak Hypodermic luer slip syringe 1 ml (syringe for clozapine injection)	Becton, Dickinson and Company, Franklin Lakes (New Jersey), USA
Dumont Mini Forceps – Inox Style 3 (Small forceps)	Fine Science Tools GmbH, Heidelberg, Germany
Dumont Mini Forceps – Inox Style 5 (Small forceps, smaller tip than Inox style 3)	Fine Science Tools GmbH, Heidelberg, Germany
Feather stainless steel blade (surgical blade)	pfm medical ag, Cologne, Germany

---

Hypodermic Needles BD Microlance 30 Gauge (0,3 mm, yellow) for subcutaneous injection of Ringer's solution and anesthesia	Becton, Dickinson and Company, Franklin Lakes, (New Jersey), USA
Microscope cover slips 24x60 mm	Gerhard Menzel Glasbearbeitungswerk GmbH & Co. KG, Braunschweig, Germany
Microscope slides 76x26 mm	Gerhard Menzel Glasbearbeitungswerk GmbH & Co. KG, Braunschweig, Germany
Noyes Spring Scissors (Large spring scissors)	Fine Science Tools GmbH, Heidelberg, Germany
Parafilm	Brand GmbH & Co. KG, Wertheim Germany
Pipettes, pipette tips and tubes (2ml and 1,5 ml)	Eppendorf AG, Hamburg, Germany
Tissue Tek Cryomold Standard, 25x20x5 mm	Sakura Finetek Europe B.V., Alphen aan den Rijn, The Netherlands
Vannas-Tübingen Spring Scissors (Small angled spring scissors)	Fine Science Tools GmbH, Heidelberg, Germany
<b>Technical devices</b>	<b>Retailer</b>
Leica CM1850 cryostat	Leica Microsystems GmbH, Wetzlar, Germany
Olympus IX71 inverted fluorescence microscope	Olympus GmbH, Hamburg, Germany
T/Pump (Heating pad)	Gaymar Industries, Orchard Park (New York), USA

---

Vortex-Genie 2	Scientific Industries, Inc., Bohemia (New York), USA
<b>Software</b>	<b>Retailer</b>
Adobe Illustrator	Adobe Systems Inc., San Jose, California, USA
CatWalk XT	Noldus, Wageningen, Netherlands
ClustVis	<a href="https://biit.cs.ut.ee/clustvis/">https://biit.cs.ut.ee/clustvis/</a>
Graphpad Prism	GraphPad Software, La Jolla, California, USA
Heatmapper	<a href="http://www.heatmapper.ca/">http://www.heatmapper.ca/</a>
Inkscape	The Inkscape Project, <a href="https://inkscape.org/">https://inkscape.org/</a>
Microsoft Office (Powerpoint, Excel, Word)	Microsoft Corporation, Redmond, Washington, USA

### 3.2 Experimental animals

Experiments were performed on male adult animals of the transgenic mouse lines Vglut2-Cre (The Jackson Laboratory; 6J.129S6(FVB)-Slc17a6tm2(cre)Lowl/Mwar) and Vgat-Cre (The Jackson Laboratory; 6J.129S6(FVB)-Slc32a1tm2(cre)Lowl/Mwar). In these mice, the expression of the enzyme cre recombinase is coupled to the expression of VGLUT or VGAT.

Mice were 8-12 weeks old at the beginning of the experiment and had stable weights between 22-28 g. They were kept in groups of maximal five mice in Type-II-cages (350 cm<sup>2</sup> x 14 cm; Tecniplast, Hohenpreißenburg, Germany) on an IVC rack system in the animal facilities of the institution. Food (“Maus” from Ssniff, Sost, Germany) and water were supplied *ad libitum*; tubes for activity were placed in each cage. Mice were held at a day and night light cycle of 12 h each and were checked regularly by trained

---

caretakers. All procedures were in conformity with institutional guidelines and approved by the Animal Study Committee of the Regierung von Oberbayern.

### **3.3 Methods**

#### **3.3.1 Pharmacological inactivation of neurons using DREADDs**

In order to temporarily silence neurons of the gigantocellular nucleus, I used Designer Receptors Exclusively Activated by Designer Drugs (DREADDs). DREADDs are chemically engineered G-protein coupled receptors, that respond exclusively to a synthetic agent and trigger intracellular signaling with different effects (Roth, 2017). For this experiment, I used the hM4D(Gi)-variant, which induces decreased firing and therefore, silencing of neurons. Its ligand was initially thought to be clozapine-N-oxide, though it was demonstrated, that it is endogenously metabolized to clozapine mediating the effect (Gomez et al., 2017). Thus, I decided to use clozapine (Sigma Aldrich) as a drug and chose a concentration of 0.1 mg/kg diluted in saline, based on pharmacokinetic data proving its efficacy and safety (Gomez et al., 2017). Using this approach, animals served as their own control. After behavioral baseline acquisition, mice were injected intraperitoneally with clozapine and then tested again.

#### **3.3.2 Viral vector for DREADD transmission and labeling**

To express the DREADDs and visualize the coexpressed fluorescence in specific subpopulations of neurons, I used the Cre-loxP system in transgenic mice in combination with a viral vector. This allowed me to virally silence and label either glutamatergic or gabaergic neurons exclusively at the injection site of the virus. When presented with an inverted, double floxed gene of interest (GOI), as I used for the DREADDs, cre recombinase flips it, so that the GOI is now able to express its protein product. It allowed me to express DREADDs and a red fluorescent protein (mCherry) to a specific subpopulation of neurons at a specific location (Figure 12). For this, I used the rAAV-hSyn-DIO-hM4D(Gi)-mCherry (Addgene). Being an adeno-associated virus, it is highly tolerable, non-immunogenic, persistent and rapid in its ability to infect neurons (Bedbrook et al., 2018). To ensure a sufficient spread in the region of interest, first trials were conducted 14 days post virus injection (dpi).

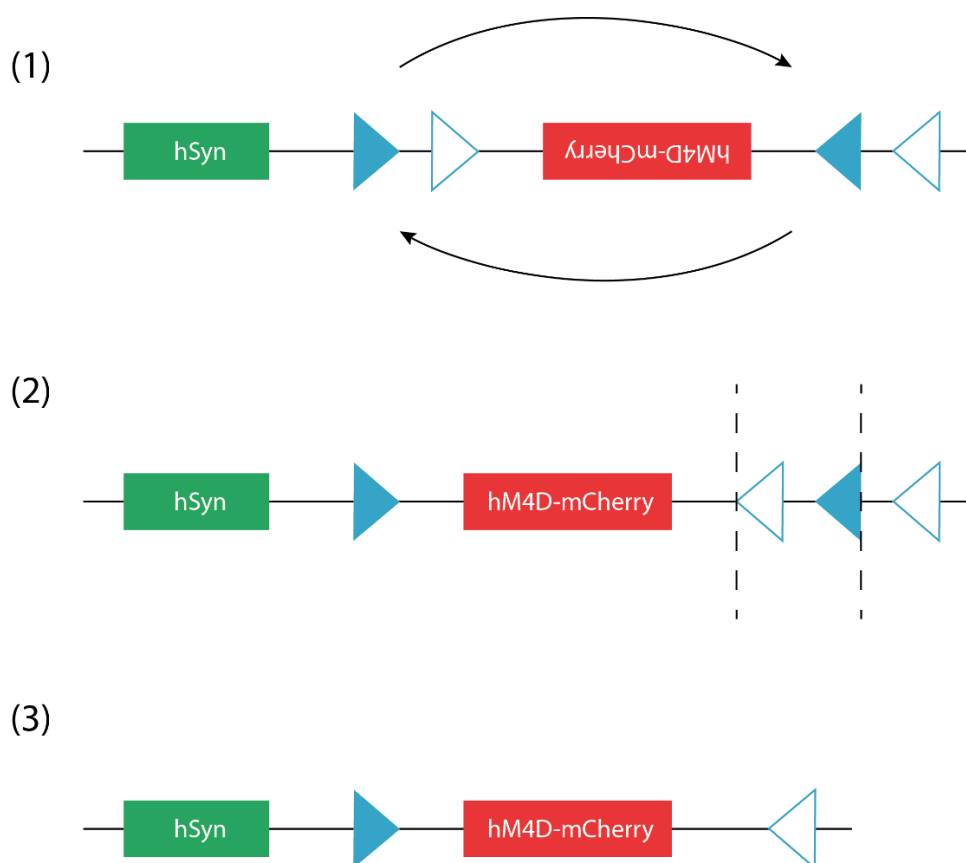


**Figure 12: Cre-loxP system.** Shown is a part of the plasmid of the rAAV8-hSyn-DIO-hM4D(Gi)-mCherry. The inverted GOI (red box) is flanked by two loxP sites on each side (arrows). (1) In presence of cre recombinase, facing loxP sites (arrows of the same color) lead to an inversion of the GOI. (2) Unidirectional loxP sites lead to a deletion between them. (3) The GOI is now steadily expressed in the plasmid. hSyn: human Synapsin promoter.

### 3.3.3 Virus injection

Viral injections of the rAAV8-hSyn-DIO-hM4D(Gi)-mCherry (Krashes et al., 2011) to the gigantocellular nucleus to transfer the DREADDs and label the neurons were performed under isoflurane anesthesia. After cranial fixation of the mice, stereotaxic injections were performed at -6.48 mm caudal to bregma. A volume of 0.5  $\mu$ l was injected to the target area of either side over a time of 10 minutes, before the needle was slowly retracted. Success and precision of the injections were later assessed by fluorescent microscopy after preparation of the tissue (Figure 13). No animal had to be excluded from the experiment due to misplaced injection. However, one animal of the VGAT group was excluded because of unknown premature death.

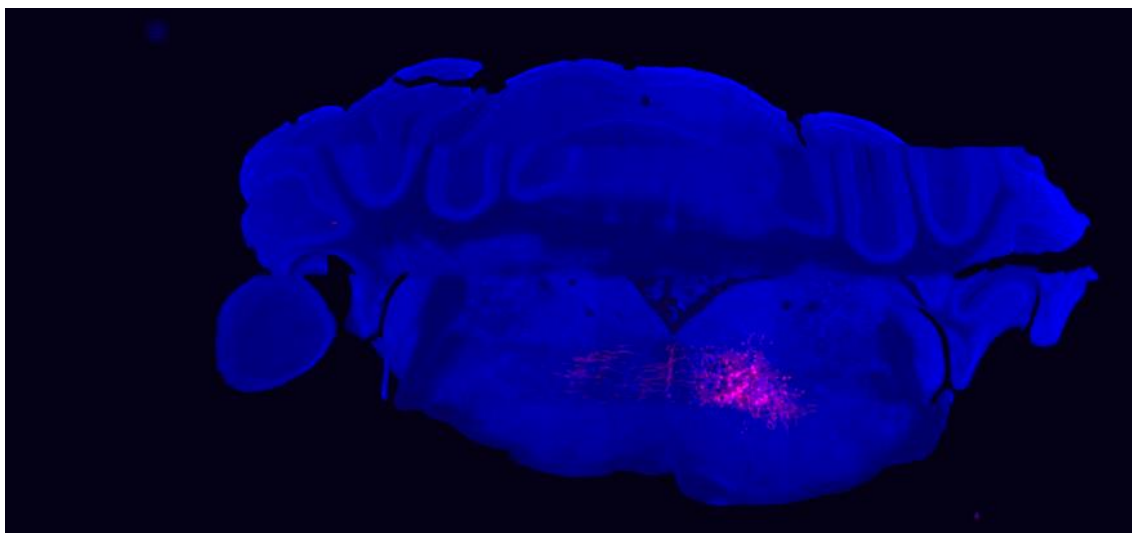


**Figure 13: Example picture of a virus injection in the NRG.** Unilateral injection of rAAV8-hSyn-DIO-hM4D(Gi)-mCherry (red) in the NRG, approximately -6.48 mm from bregma, 21 dpi. Mice in this experiment received a bilateral injection.

### 3.3.4 Tissue processing

#### Transcardial Perfusion

Mice were fully anesthetized using isoflurane (AbbVie, North Chicago, USA). When neither movements nor breathing could be detected, they were pinned on their back to a platform by their extremities. The heart and abdomen were prepared by cutting open the skin, peritoneum and bony thorax with a scissor. Then, a butterfly cannula attached to a micropump (20  $\mu$ l/s; ISMATEC, Wertheim, Germany) was inserted into the left ventricle; the right atrium was opened up with the scissor to create an outflow. To prevent coagulation, 0.1% Heparin-sodium solution (Ratiopharm, Germany) in 1x phosphate-buffered saline (PBS) was pumped through the circulatory system, until visually no more blood came out of the right atrium. Subsequently, about 25 ml of 4% Paraformaldehyde (PFA) in 0.1 M phosphate buffer (PB) was applied to the system in order to fixate the tissue. Success of perfusion was assessed by decolorization of the liver, muscle stiffness and a “dancing” tail. When the criteria were satisfyingly fulfilled, the head and part of the spinal cord were dissected *en bloc* and placed in post fixation 4% PFA for 24 h at 4°C.

---

## **Microdissection**

To isolate the brain and prepare it for cutting, it had to be removed from surrounding tissue. Under a microscope, the cranium was opened by a sagittal cut with a scissor. Then, using forceps, parietal and occipital bones of the cranium as well as dorsal parts of the spine were cautiously broken away to expose the brain and cranial parts of the spinal cord. Exposed parts were bluntly freed from connective tissue including the dura mater and were extracted as a whole. Finally, the tissue was placed in a 30% Sucrose (Sigma, cat-S0389) 1x PBS solution for 48 h. For long term storage, tissue was placed in a 0.1% sodium azide (NaN<sub>3</sub>) solution in 1x PBS.

## **Cryosection & Tissue Preparation**

To prepare the brainstem for further analysis, it had to be cut into slices and mounted on slides. For this, the spinal cord was cut off from the brain with enough space to ensure an intact brainstem. The brain was then covered in an optimal cutting temperature medium (O.C.T., Tissue-Tek, Sakura, Finetek, USA) and put in the freezer at -20°C for at least 20 min. When completely frozen, the brainstem was cut coronally in 50 µm slices with a Leica CM 1850 cryostat. Sections were immediately mounted on subbed slides (0.5% gelatin and 0.05% chromium potassium sulfate coating) to conserve anatomical order. Lastly, they were dried overnight at room temperature.

### **3.3.5 Behavioral tests**

For every test, animals were habituated on three days in the week prior to the first trial. Behavioral trials were conducted on 14, 18 and 25 days post virus injection (dpi), as the timeframe of 2-4 weeks post injection to ensure sufficient viral spread and safety was shown to produce reliable data (Krashes et al., 2011; Asboth et al., 2018; Bradley et al., 2019). One data point consisted of the mean of one subject on one day of testing. On a day of testing, after baseline testing had been completed for every subject, clozapine was injected intraperitoneally to mice following a preset time schedule, in order to ensure equal doses for the same test considering pharmacokinetics. Testing always started at 45 min after i.p. injection and ended at 150 min.

## **Rotarod**

To assess locomotor activity, I used the rotarod test (Ugo Basile, Italy; Hamm et al., 1994). Mice are put on a rotating rod around 10 cm from the ground. After

---

habituation, they start walking naturally on it to prevent a fall. The measured parameter was the time latency to fall. In fixed speed mode, mice are tested with a fixed speed of 20 rounds per minute until a maximum of 120 s is reached. In accelerated speed mode, mice are tested with accelerating speed of 2-40 rounds per minute until a maximum of 120 s is reached. A total of three rounds with pauses of 2 min in between were tested for each day.

### **Ladder rung**

For separated measurement of hindlimb and forelimb placement and coordination, I used the ladder rung as previously described (Metz & Whishaw, 2009). In this test, mice walk on a horizontal metal ladder with rungs 1 cm apart from each other (regular ladder rung) or with rungs 1 or 2 cm apart from each other in a random pattern, that is different on each day (irregular ladder rung). Walls of plexiglass on both sides force mice to go in one direction. Videotaped trials were then watched frame by frame by a blinded observer, who scored them. One point was given for a missed or a slipped step and points were summed for all limbs. One trial consisted of the mouse walking the ladder back and forth with a total of three trials a day.

### **CatWalk gait analysis**

Evaluation of gait and interlimb coordination was conducted using the CatWalk XT™ system (Noldus; Hamers et al., 2006). In short, the catwalk is a narrow, transparent walkway, that is being filmed from beneath. A light source highlights the parts of the animal having contact with the platform, mainly the paws. When the mouse walks across the walkway, its paw placements are tracked and recorded. For reproducibility, walks were only valid, if they fulfilled specific criteria. I set a minimum run duration of 0.5 s, a maximum run duration of 4 s and a maximum speed variation of 60% of maximum speed, to ensure consistent walking without interruption. For each day of testing, three runs per animal were recorded and used for analysis. After acquisition, a blinded observer identified the paw prints and ruled out non-paw structures using the custom CatWalk software. Based on this data, the software automatically calculates different parameters from which I chose the following for best assessment of mentioned functions.

### ***Regularity Index***

The regularity index (RI, in %) is a measure of interlimb coordination, which analyzes stepping patterns based on the sequence of paw placements. It is defined as the number

of normal step sequence patterns (NNSP) relative to the total number of paw placements (PP).

$$\text{Regularity index} = \frac{\text{NNSP} \times 4}{\text{PP}} \times 100\% \quad (1)$$

A NNSP is defined by the software as one of the major step sequences mice use (Table 1). Therefore, physiological mice have a RI of 100%, as they use physiological step sequence patterns, whereas mice with deficits regarding coordination in SCI models tend to make steps out of step sequence patterns, resulting in a lower RI (Vrinten and Hamers, 2003; Koopmans et al., 2005; Gabriel et al., 2007). An example of the analysis is given in Figure 14.

**Table 1: List of normal step sequence patterns recognized by the software.**

Cruciate	Pattern Ca	RF - LF - RH - LH.
	Pattern Cb	LF - RF - LH - RH
Alternate	Pattern Aa	RF - RH - LF - LH
	Pattern Ab	LF - RH - RF - LH
Rotate	Pattern Ra	RF - LF - LH - RH
	Pattern Rb	LF - RF - RH - LH

RF: right forelimb. LF: left forelimb. RH: right hindlimb. LH: left hindlimb.

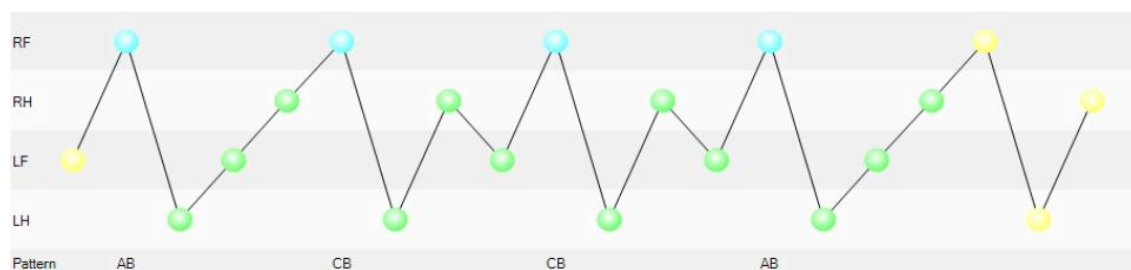


**Figure 14: Exemplary analysis of stepping patterns in the CatWalk software.** The animal had four normal stepping patterns. All patterns start with the right front paw (blue dot). The first paw print and the last three are not taken into account (yellow dots). The number of accounted steps is 16. Regularity Index is 100%. RF: right forelimb. LF: left forelimb. RH: right hindlimb. LH: left hindlimb.

### *Couplings*

Couplings, sometimes also referred to as phase dispersions or phase lags, is a measure of more subtle differences in interlimb coordination. It describes the temporal relationship between placement of two paws within a step cycle in percent. One paw serves as an anchor, while the other one is the target.

$$\text{Couplings} = \frac{\text{anchor to target}}{\text{step cycle}} \times 100\% \quad (2)$$

anchor to target: minimal time from target to next anchor in s

step cycle: time of the step cycle between two anchors in s, that includes the interval anchor to target

In order to generate consistent values, a target paw always relates to its nearest anchor paw, so that values range from 0%, when paws are simultaneously placed, to 50%, when paws are alternately placed. Depending on which paws are anchor and target, physiologic Couplings values are either close to 0% or 50% (Batka et al., 2014; Caballero-Garrido et al., 2017). An example of a calculation of Couplings is given in Figure 15.

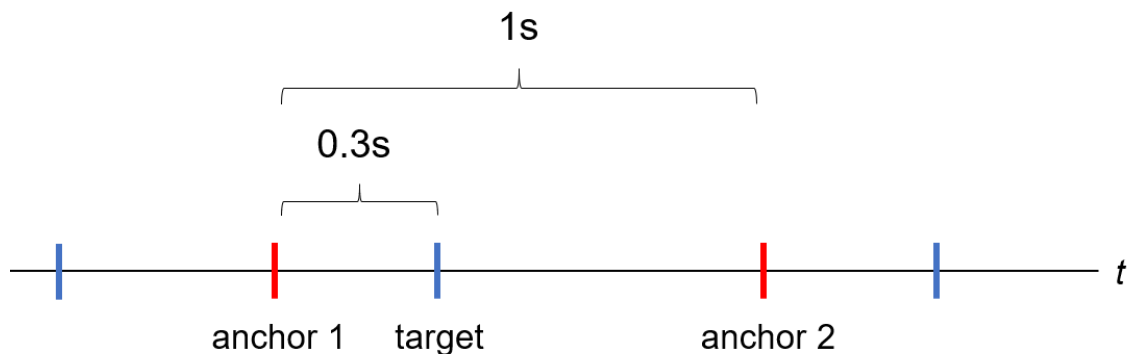


**Figure 15: Exemplary calculation of Couplings.** The temporally closest anchor of the target paw is anchor 1. The time from anchor 1 to target is 0.3 s. The step cycle including this interval ranges from anchor 1 to anchor 2 with a total time of 1 s. Couplings is therefore 30%. Red lines: right forelimb placement. Blue lines: left forelimb placement.

### *Base of support*

The base of support (BOS) is the distance in mm between either the forelimbs (BOS-FL) or the hindlimbs (BOS-HL) and is measured perpendicularly to the direction of walking

(Figure 16). It is an indicator of posture and balance during locomotion. After SCI, BOS-FL decreases or remains unaltered, while BOS-HL increases (Hamers et al., 2001; van Meeteren, 2004; Petrosyan et al., 2013).

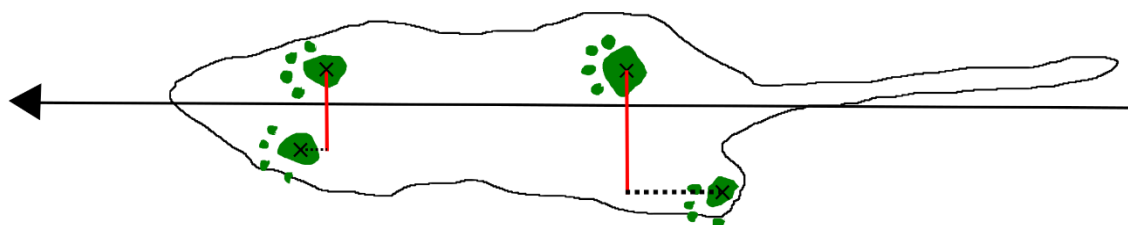


**Figure 16: Schematic camera view of a mouse on the CatWalk.** Arrow indicates movement direction. Red lines represent BOS-FL and BOS-HL.

### *Principal component analysis*

Principal component analysis (PCA) is a multivariate statistical analysis to reduce dimensionality with minimal information loss in large data sets with correlating parameters (Courtine et al., 2009). It transforms a given coordinate system with  $n$  dimensions to a new coordinate system, on which variance between axes is maximized. Aim of this mathematical transformation is to analyze few principal components instead of all  $n$  dimensions or a selection of dimensions. As the CatWalk analyzes 177 different parameters (177 dimensions) with high correlations between them, I performed a PCA on its data using the online software ClustVis (Metsalu and Vilo, 2015). In every group, principal component 1 and 2 together accounted for about 50% of all variance in the data sets, demonstrating the high correlations between the CatWalk parameters. Principal component 1 and 2 were then statistically analyzed and plotted in a two-dimensional coordinate system. Factor loadings, showing the correlation between single parameters and a principal component, were visualized using the online software Heatmapper (Babicki et al., 2016).

### **3.3.6 Data analysis**

All datasets were analyzed and plotted as graphs using Prism 7.00 for Windows (GraphPad Software). Considering that some of the tests contain cutoff points and taking into account the results of D'Agostino & Pearson normality tests, I assumed a non-Gaussian distribution for the following parameters: fixed and accelerated rotarod,

---

regularity index and Couplings. On these parameters I performed non-parametric Wilcoxon matched-pairs tests with the method of Pratt. On all other parameters (including principal component scores of the PCA), I performed two-tailed paired Student's t-tests. Significance level was set as  $P < 0.05$ . Results are either reported in box plots and whiskers (calculated after Tukey) or as means  $\pm$  standard error of the mean (SEM). One datapoint represents the mean of three trials of any test of one subject at one time point.

## 4 Results

### 4.1 Behavioral analysis of mice after silencing of neural subpopulations of the NRG

To determine the functional contributions of neural subpopulations of the NRG to general locomotion in mice, I conducted a behavioral loss-of-function experiment with the usage of DREADDs, in order to be able to reversibly silence target neurons by pharmacological intervention before behavioral analysis. To transmission DREADDs to the NRG of mice, I stereotactically injected the virus AAV-hSyn-DIO-hM4D(Gi)-mCherry bilaterally into the NRG of mice of experimental groups (Figure 17). I used four mice of the transgenic mouse line Vglut2-Cre and three mice of the mouse line Vgat-Cre to specifically target glutamatergic and gabaergic subpopulations, respectively (Table 2). The control group consisted of four mice of the mouse line Vglut2-Cre, which received a saline solution instead of the virus. On days 14, 18 and 25 post virus injection, animals were behaviorally tested on the rotarod, the ladder rung and the CatWalk before and after intraperitoneal application of clozapine (Figure 18). As test subjects served as their own baseline and results were analyzed by either Wilcoxon matched-pairs tests or paired Student's t-tests, results are presented either as box plots or means together with individual data points. For every new pharmacological silencing at different time points represented different conditions, I considered every time point a data set on its own, resulting in group sizes of 12 for the CTRL and VGLUT group and 9 for the VGAT group. Following are the results of the different behavioral tests.

**Table 2: Definition of the different groups of the experiment.**

<b>Group</b>	<b>Mouse line</b>	<b>Virus</b>	<b>Drug administered</b>	<b>Effect after baseline testing</b>
VGLUT	Vglut2-Cre	Yes	Clozapine	Inhibition of glutamatergic neurons
VGAT	Vgat-Cre	Yes	Clozapine	Inhibition of gabaergic neurons
CTRL	Vglut2-Cre	No	Clozapine	None

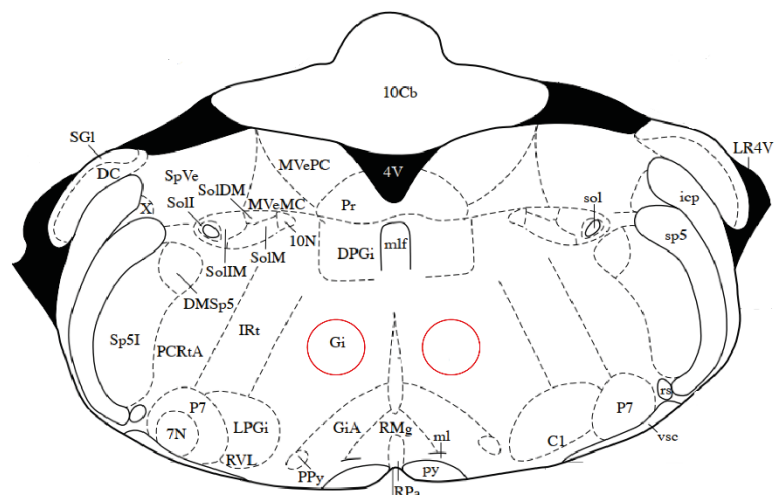


**Figure 17: Viral injection sites.** The virus AAV-hSyn-DIO-hM4D(Gi)-mCherry was bilaterally injected into the NRG of the ReST, -6,48 mm from bregma. Shown is a corresponding coronal brainstem section. Gi: NRG. Red circles indicate injection sites. Adapted from Paxinos and Franklin, 2001.

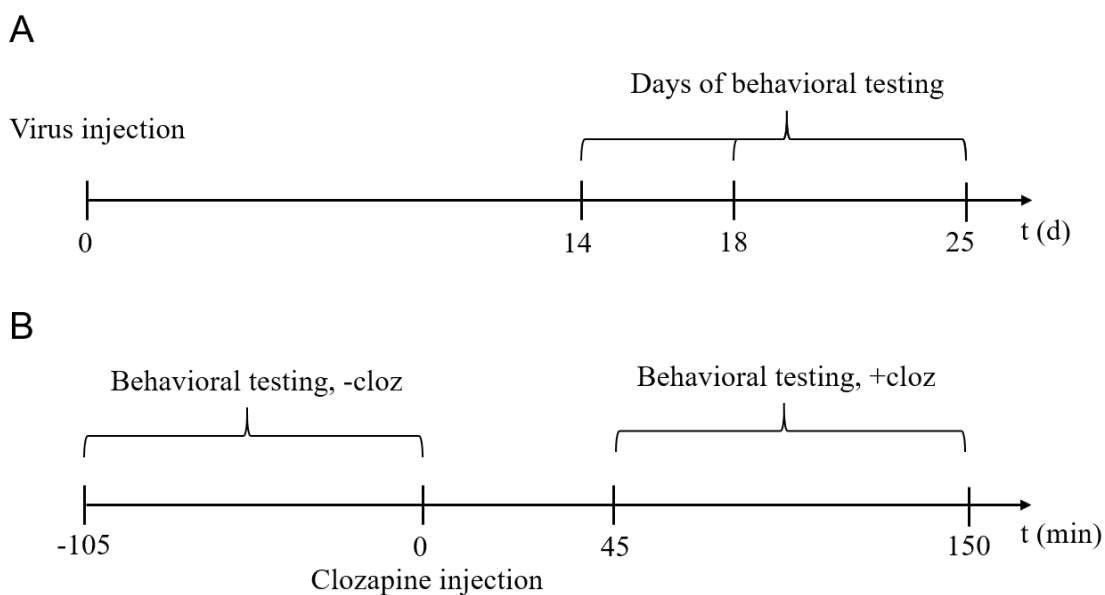


**Figure 18: Experimental setup.** **A** | Experimental setup. Animals were behaviorally tested 14, 18 and 25 days post viral injection. **B** | Time schedule of one day of testing. Subjects were tested before administration of clozapine for baseline acquisition and afterwards. -cloz: baseline without clozapine. +cloz: after clozapine injection.

## Rotarod

Because the rotarod is a widely used method for the assessment of behavior in rodent SCI models, I selected it as an indicator of general locomotion in my study. Walking ability on a rotating rod is more of an undifferentiated parameter, which evaluates coordination, balance and overall walking capacity, which makes it indeed vague in terms of the specificity of impaired motor functions. However, for the same reason it is very sensitive and a good tool to screen for any deficits regarding locomotion. Testing could only detect significant decline in performance in the VGAT group in the fixed rotarod test (Figure 19). This could not be seen in the accelerated mode, though. As general locomotion per se does not seem to be consistently impaired, one could suspect an impairment of speed dependent locomotion control.

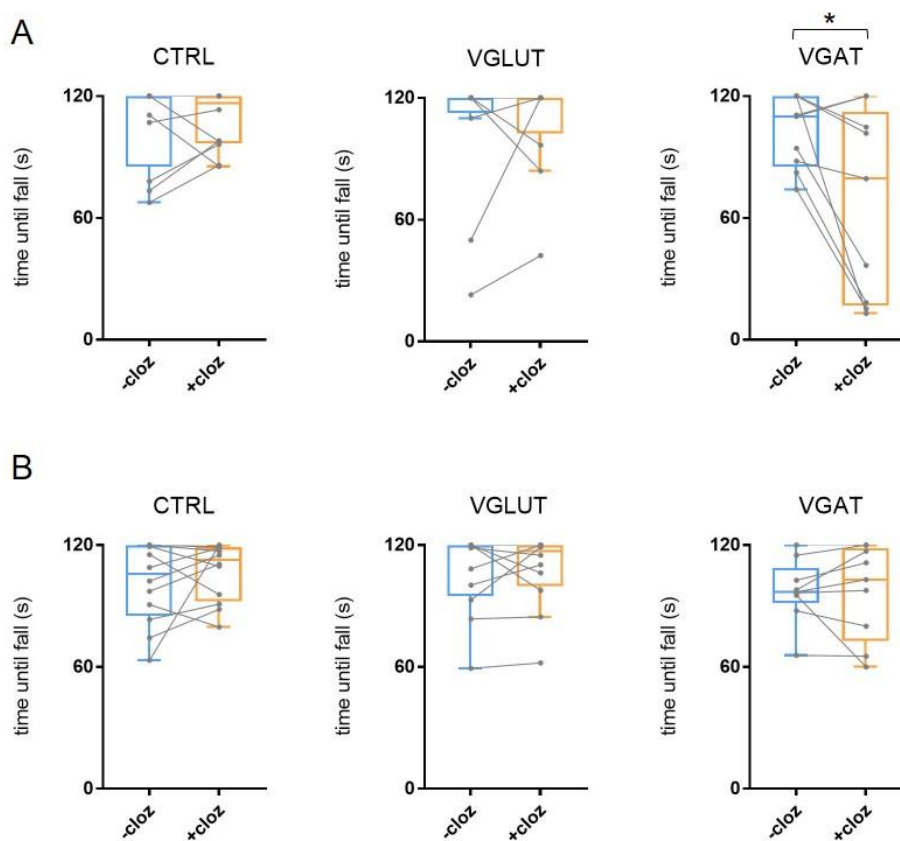


**Figure 19: Fixed and accelerated rotarod results.** **A** | Fixed rotarod. **B** | Accelerated rotarod. -cloz: baseline without clozapine. +cloz: after clozapine injection. Grey dots and lines: paired data points as means of one subject at one time point. Colored box plots and whiskers: median as line inside box, 25th and 75th percentile as lower and upper box boundary, whiskers calculated after Tukey, median and boundaries might fall together. \* $P < 0.05$ . nCTRL = 12, nGLUT = 12, nVGAT = 9.

## Ladder rung

The ladder rung, regular and irregular, is an assessment of coordinated paw placement and voluntary motor control and is therefore often used for CST models. Yet, since balance and interlimb coordination also influences paw placement, I applied it to the ReST. The results given do not show any significances, indicating no adherent effects of NRG silencing regarding mentioned locomotion qualities (Figure 20). It has to be noted, that baseline differences among groups are probably attributed to the different mouse lines used. The CTRL group and the VGLUT group were of the same mouse line and share similar baseline values.

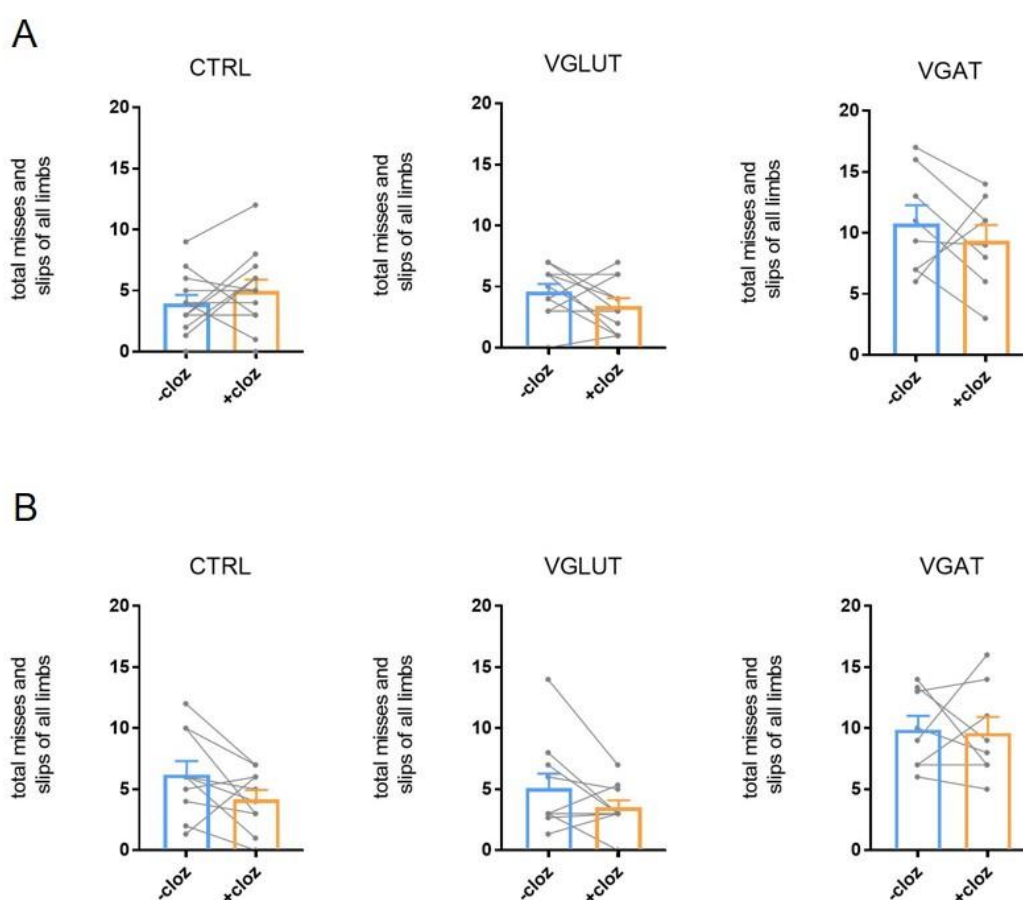


**Figure 20: Regular and irregular ladder rung results.** **A** | Regular ladder rung. **B** | Irregular ladder rung. -cloz: baseline without clozapine. +cloz: after clozapine injection. Grey dots and lines: paired data points as means of one subject at one time point. Colored bars: means  $\pm$  SEM. \* $P < 0.05$ . nCTRL= 12, nGLUT = 12, nVGAT = 9.

---

## **CatWalk**

The Catwalk is an automated gait analysis system that allows the assessment of motor function and coordination in rodents. Mice walk across an illuminated glass platform while a video camera records from below. Gait related parameters are reported for each animal.

### ***Principal component analysis***

The CatWalk software automatically analyzes 177 different gait parameters with high correlations between them. I performed a principal component analysis (PCA) on the data set in order to (1) maximize information gain and (2) avoid a selection bias. PCA is a multivariate statistical analysis transforming  $n$  parameters with a coordinate system of  $n$  dimensions to a new coordinate system, on which the variance between the axes is maximized. Neither principal component 1 nor principal component 2, which account for close to 50% of all variance in all of the parameters, show significant differences after clozapine injection (Figure 21). This strongly suggests no major gait alterations after NRG silencing. Furthermore, after clustering the parameters in three main categories (paw print shape, paw placement and interlimb coordination; Figure 22), I selected additional parameters, indicating paw placement and interlimb coordination, for further analysis based on their correlation with principal component 1 (Figure 22). Thus, these parameters, which are regularity index, Couplings and base of support, are highly representative of interlimb coordination.

### ***Regularity index***

The regularity index is a parameter that I chose as an index of interlimb coordination. In unaffected mice, its values are close to 100%. In all three experimental groups, there was no significant decline of the regularity index detectable after clozapine injection (Figure 23). This means, that no major abnormalities in the stepping pattern of subjects occurred due to silencing of the NRG. Although the regularity index is a highly consistent parameter and susceptible to spinal cord injuries, changes are not gradually quantified, but stepwise, which has led me to the conclusion, that slight deficits in interlimb coordination might not be detected. Hence, I decided to analyze Couplings, a parameter, whose scaling of values allows for more sensible differentiation.

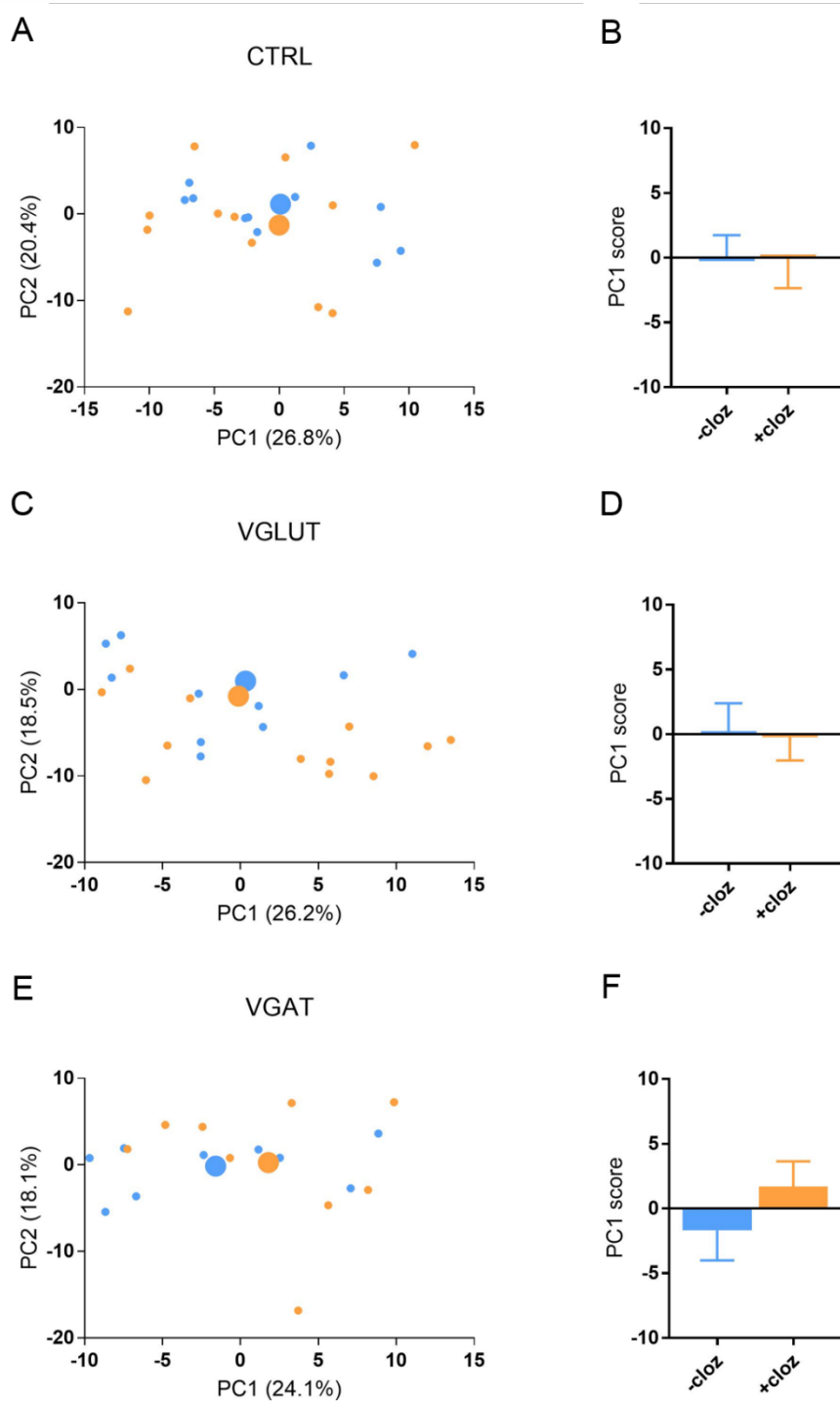


**Figure 21: CatWalk principal component analysis results.** A, C, E | Principal component 1 and 2 scores of different groups. Notice, that the distance between means is short. Percentage value of a component indicates the percentage of variance represented by its component. B, D, F | Principal component 1 results of different groups. None of them are significant. Blue dots: individual data points, baseline. Orange dots: individual data points, after clozapine injection. Big dots: means. Blue and orange bars: means  $\pm$  SEM. \* $P < 0.05$ . nCTRL = 12, nVGLUT = 12, nVGAT = 9.

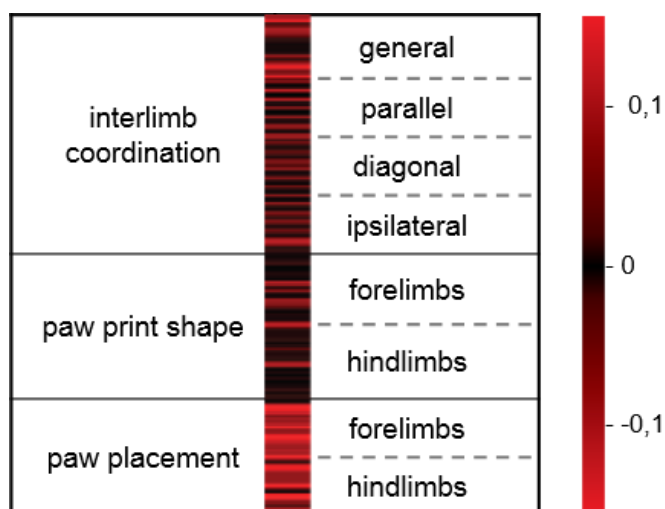


**Figure 22: Factor loadings of PC1 of CTRL.** Exemplary demonstration of factor loadings of principal component 1 of the CTRL group as colored bar. Every line in the bar represents one parameter of the CatWalk; its color represents its correlation to principal component 1. Colored gradient on the right shows color code used. The factor loadings show a high relation between CatWalk parameters and principal component 1.

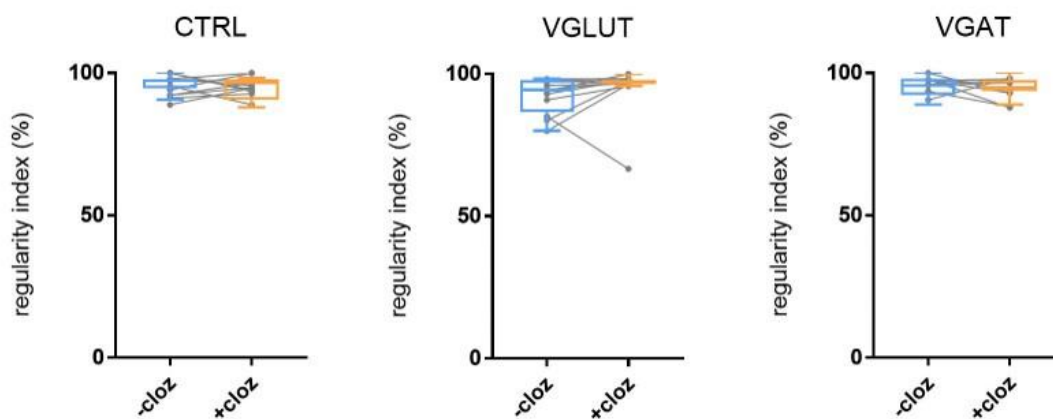


**Figure 23: Regularity index results.** Regularity index. -cloz: baseline without clozapine. +cloz: after clozapine injection. Grey dots and lines: paired data points as means of one subject at one time point. Colored box plots and whiskers: median as line inside box, 25th and 75th percentile as lower and upper box boundary, whiskers calculated after Tukey, median and boundaries might fall together. \* $P < 0.05$ . nCTRL = 12, nGLUT = 12, nVGAT = 9.

---

### ***Couplings***

In contrast to the regularity index, which examines step sequences, Couplings measures the temporal relation of single steps towards each other within a step cycle. For this reason, it might be able to unmask minor deficits of interlimb coordination, that the regularity index was not able to adequately present. I analyzed a total of four Couplings, two with an anchor and target from crossed limbs and two with an anchor and target from parallel limbs (Figure 24). These are Couplings between left hindlimb and right forelimb (LH-RF), right hindlimb and left forelimb (RH-LF), right forelimb and left forelimb (RF-LF) and right hindlimb and left hindlimb (RH-LH). Couplings of crossed limbs tend to be near 0% in healthy mice, while Couplings of parallel limbs tend to be near 50% in healthy mice. The results presented show no significant differences between the control group and the test groups, with baseline values within the range of expectance. In accordance with the results of the regularity index, inactivation of NRG subpopulations does not seem to affect interlimb coordination.

### ***Base of support***

Base of support, the width of a mouse's stand, is a measure of posture and balance during locomotion and is measured separately for the forelimbs and the hindlimbs (

Figure 25). After clozapine injection, it remained unaltered in the test subjects and did not demonstrate significance. It can be concluded, that the NRG probably does not play a crucial role in posture and balance during general locomotion.

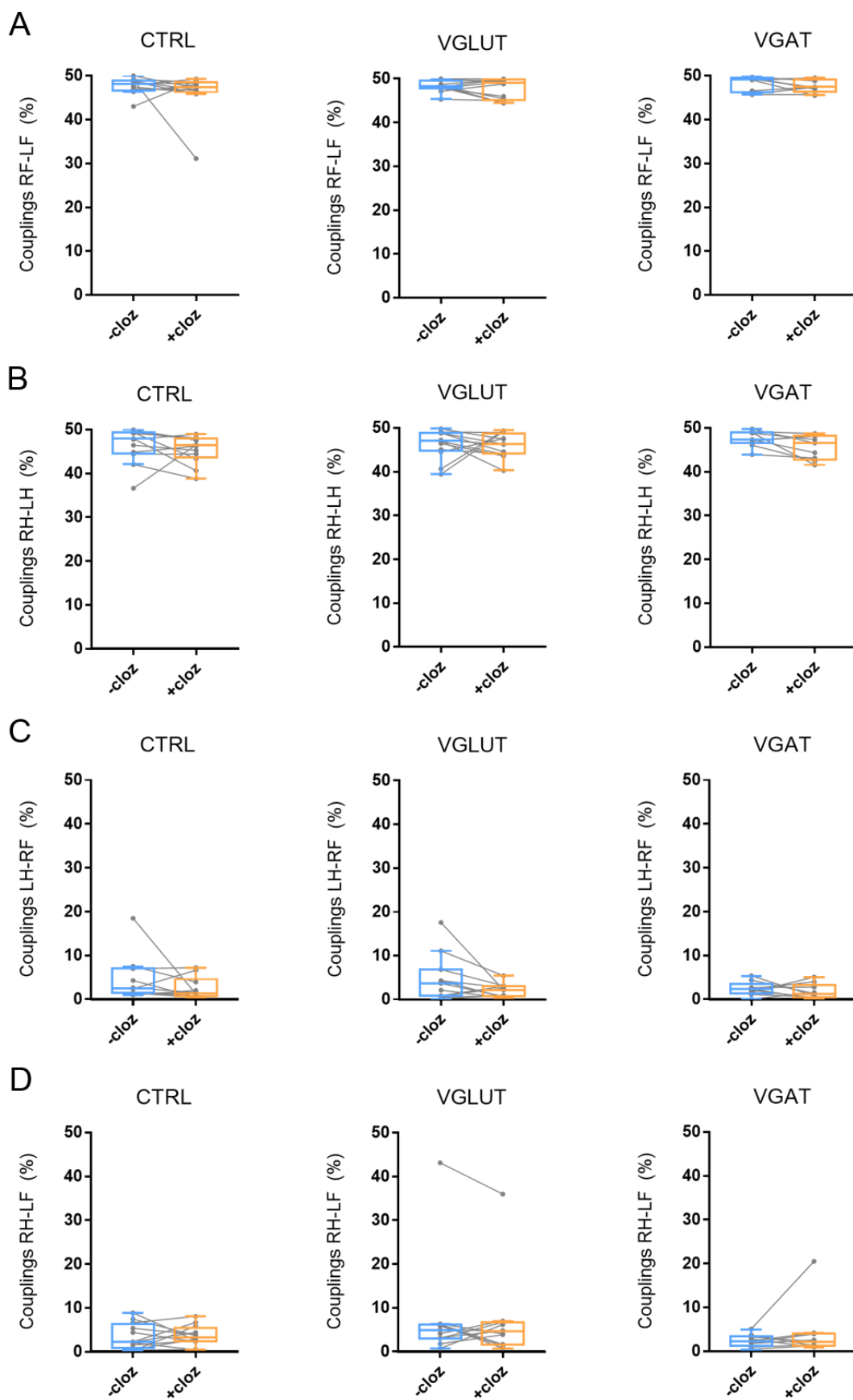


**Figure 24: Couplings results.** **A** | Couplings between right forelimb and left forelimb. **B** | Couplings between right hindlimb and left hindlimb. **C** | Couplings between left hindlimb and right forelimb. **D** | Couplings between right hindlimb and left forelimb. -cloz: baseline without clozapine. +cloz: after clozapine injection. Grey dots and lines: paired data points as means of one subject at one time point. Colored box plots and whiskers: median as line inside box, 25th and 75th percentile as lower and upper box boundary, whiskers calculated after Tukey, median and boundaries might fall together. \* $P < 0.05$ . nCTRL = 12, nGLUT = 12, nVGAT = 9.

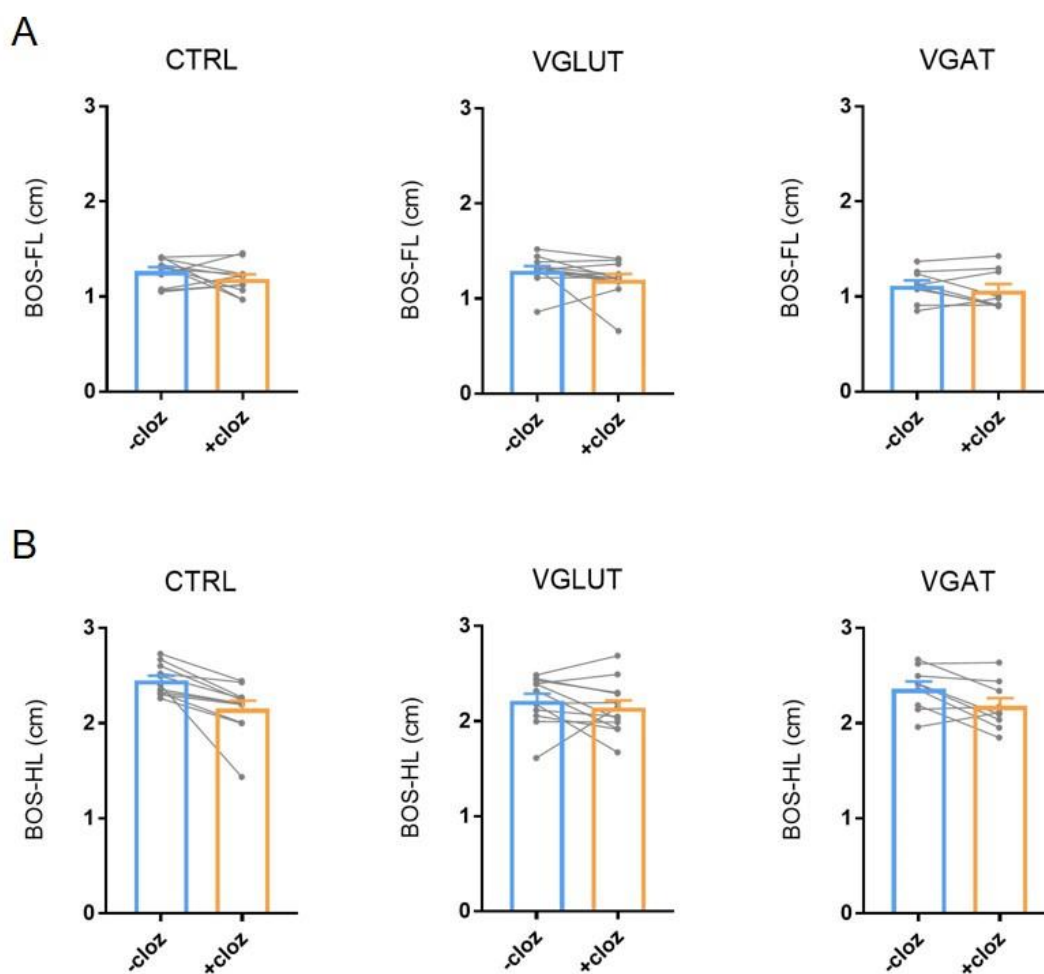


**Figure 25: Base of support results.** **A** | Base of support of forelimbs. **B** | Base of support of hindlimbs. -cloz: baseline without clozapine. +cloz: after clozapine injection. Grey dots and lines: paired data points as means of one subject at one time point. Colored bars: means  $\pm$  SEM. \* $P < 0.05$ . nCTRL = 12, nGLUT = 12, nVGAT = 9.

---

## **5 Discussion**

### **5.1 Summary**

The aim of this experiment was to (1) to identify the NRG's physiologic contribution to general locomotion, (2) to identify functional differences of neural subpopulations and (3) to evaluate whether further SCI research should primarily concentrate on the NRG as a major nucleus of the ReST or whether additional nuclei should be investigated in the frame of the control of locomotion by the reticulospinal tract. Behavioral analysis of different aspects of motor functions involved in general locomotion and gait could not show any significant changes after functional silencing of the NRG and thus question an essential involvement of the NRG in locomotion. Hence, no conclusion about the relative functional contribution of different neural subpopulations of the NRG to locomotion can be drawn from this experiment. Concerning future SCI on the ReST, other nuclei of the ReST seem to be of higher or at least similar interest as the NRG.

### **5.2 Potential and limitations of used methods**

#### **5.2.1 DREADD induced silencing of neural subpopulations**

Chemogenetics is a well-established method and has been used extensively in neuroscientific experiments since its discovery. Its efficacy and our usage of it in the lab was proven by a previous study (Bradley et al., 2019). Crucial for proper silencing of regions of interest is of course proper transfection of target areas. After preparing the tissue, I evaluated the accuracy of the viral injections by fluorescent microscopy (Figure 13). Checking for labeling outside of the NRG and sufficient rostral to caudal expansion, I did not have to exclude any animals. Thus, I ruled out inadequate DREADD transmission as a source of error.

In contrast to previous DREADD experiments in our lab, I introduced clozapine instead of clozapine-N-oxide (CNO) as pharmacologic ligand, based on newly found observations, that CNO is endogenously metabolized to the more potent clozapine. The study suggests a concentration of 0.1 mg/kg clozapine for future experiments, which I adopted (Gomez et al., 2017). Concerning efficacy, it equals a concentration of 10 mg/kg CNO, which is a widely used concentration of CNO in DREADD experiments

---

(Mahler et al., 2014; Smith et al., 2017). Unspecific effects could only be observed with 1 mg/kg clozapine (Gomez et al., 2017). However, a more detailed analysis of pharmacokinetics in mice in a follow-up experiment revealed a short interval of 15 min to reach effective doses and a fast decline, with much lower doses being in effect at 60 min after i.p. injection of clozapine. The recommended dose here was 0.2-0.5 mg/kg clozapine (Jendryka et al., 2019). Another experiment though, that used the same approach as I did, could generate sufficient silencing with the hM4Di and 0.1 mg/kg clozapine (Zhou et al., 2018).

I conclude on the one hand, that my choice of concentration was probably sufficient for adequate silencing, but on the other hand and in light of very recent publications, that were not known at the time of my laboratory work, that my timeframe of testing between 45-150 min after i.p. injection might have been too long. It is not certain, if adequate silencing was still effective at late time points, which could conceivably explain the lack of significant changes observed in my behavioral experiments. It should be noted, though, that I changed the sequence of behavioral tests with every day of testing, so that if a significant impact of clozapine on a test was missed due to low concentrations, it should have been observable on a different day with a different sequence (and ergo a different concentration). Results of different time points were largely consistent, however.

As this experiment did not verify the efficacy of the method used and produced solely negative results, failure of the method cannot be excluded. Yet, its similarity in set-up as previously mentioned studies make it rather unlikely.

Unspecific effects or interactions of clozapine regarding locomotion were initially shown only at much higher concentrations than 0.1 mg/kg (Gomez et al., 2017). A following study, however, could detect unspecific alterations of locomotion at a concentration of 0.01 mg/kg by expanding the time frame (Ilg et al., 2018). This finding and the longer duration of efficacy of CNO due to steady conversion has led some researchers to favor the usage of CNO again (Mahler and Ashton-Jones, 2018). Yet, rodents exhibit high variability in their endogenous CNO to clozapine conversion rates resulting in more inconsistent locomotion performances of subjects within groups of the same concentration (Malvich et al., 2018). Overall, it can be concluded, that the choice of drug should be preceded by a screening for unspecific effects of each drug with a tendency to favor CNO, if intervals of more than 60 min are needed, and to favor clozapine, if intervals are shorter. Concerning this experiment, unspecific effects of clozapine on

---

locomotion were ruled out by negative controls. For future experiments with similar set-up, CNO might be the better choice. In the long term, newly developed drugs for DREADD activation like compound 21 and perlapine could represent better solutions, if they prove to be inert (Chen et al., 2015).

### **5.2.2 Selection of behavioral tests**

Adequate behavioral testing is generally a challenging task, as most motor assessments are either very specific, subjective, non-linear or simply not sensitive enough. Additionally, motor impairments are diverse in their characteristics and depend on the injury model. As this experiment modified motor functions in a way that was not tested before, I used a battery of tests evaluating different aspects of motoric assessments in order to cover a wide range of impairments. However, it is not guaranteed, that this selection of tests would pick up the changes, if any, triggered by the DREADDs. I will further elaborate on the choice of the battery of tests and the absence (and possible necessity) of the analysis of kinematics, e.g. the tracking of joint angles through a camera system, which is a very sensible method for behavioral assessment having made its way into SCI research.

The rotarod is a well-established test for motoric assessment in rodents (Hamm et al., 1994; Loy et al., 2018). It is excellent for the analysis of general locomotion, locomotion initiation and speed dependent locomotion and was able to pick up differences in the accelerated mode. It does not evaluate any movement or stepping patterns, meaning that it is possible for mice to perform well despite impairments, through compensation.

The ladder rung is used mostly in CST injury models to assess fine paw placement, but also overground locomotion (Loy et al., 2018). It is highly sensitive and covers contrasting qualities in comparison to the rotarod, making it a good addition to it (Metz and Whishaw, 2009). A drawback is the subjectivity of its analysis, which can make it more difficult to compare between observers.

The CatWalk gives a detailed analysis of gait and movement patterns separating it from performance dependent tests like rotarod and ladder rung (Bradley et al., 2018; Loy et al., 2018). This enables it to pick up impairments, that are compensated through alternative movements and thus, do not result in a decline of specific motor performances.

---

The PCA was able to categorize the correlating parameters into the qualities paw print shape, paw placement and interlimb coordination.

Altogether, the battery of tests covers a broad range of motor functions associated with general locomotion and is, therefore, quite suitable for a screening for potential motor impairments mediated via the reticulospinal tract. However, as kinematics are widely used in SCI models and physiologic locomotion research, the question of its necessity in this experiment, particularly whether it can detect alterations not picked up by the other tests, arises (Courtine et al., 2008; Capelli et al., 2018). While kinematics could detect alterations in gait in experiments with negative rotarod and ladder rung results, the CatWalk parameters base of support and Couplings were demonstrated to be correlated to kinematic gait analyses (Zörner et al., 2010; Stroobants et al., 2013; Fiander et al., 2017). Yet, there is no direct comparison between the sensitivity of these parameters and the sensitivity of kinematic joint tracking to this date. It can be theorized, that while both methods appear to be suitable for the assessment of motoric functions directly involved in locomotion, kinematics cover a broader spectrum of possible interfering variables, including functions not directly, but indirectly involved in locomotion, like posture or muscle tone. Because of this reason, this study cannot draw conclusions concerning these qualities.

Furthermore, it could be argued, that the threshold of significant behavioral changes might be too high to be reached by silencing of single nuclei of a tract. Such concerns are easily dissolved, as numerous studies have optogenetically or chemogenetically silenced neuron populations, similar in size, of corticospinal or extrapyramidal tracts with detectable behavioral changes (Siegel et al., 2015; Asboth et al., 2018).

### **5.3 The NRG's physiologic contribution to general locomotion**

If we assume, that the behavioral tests can pick up differences due to the silencing and in consideration of the fact, that nearly all of the behavioral tests show no significant alteration after clozapine injection and subsequent neural silencing, there is doubt about the NRG playing a crucial role in the elicitation of general locomotion. According to several c-Fos experiments (c-Fos is a transcription factor and marker for recent neural activity), the NRG is definitely in use in walking mice (Bretzner and Brownstone, 2013;

---

Capelli et al., 2017). Hence, it can be assumed, that its function is either redundant or supportive, e.g. regulating muscle tone or posture.

The effects of stimulation of the NRG on muscle tone were indeed already demonstrated in an experiment using EMG recordings (Takakusaki et al., 2015). A more recent study, which combined EMG recordings and optogenetics in glutamatergic neurons of the NRG, confirmed an effect on muscle tone and additionally showed a phasic modulation of locomotion associated rhythms in the EMG. However, ongoing stimulation or inhibition was not sufficient to elicit or stop locomotion, respectively (Lemiux and Bretzner, 2019).

Another study chose a different approach and quantified c-Fos expression of different nuclei of the ReST after treadmill walking. Surprisingly, expression was not only seen in several nuclei of the ReST, but was also strongest in the lateral paragigantocellular nucleus (LPGi), not in the NRG. Then, the authors differentially stimulated the nuclei through optogenetics in Vglut2-Cre and Vgat-Cre mice, the same mouse strains I used in this experiment. Interestingly, stimulation of the NRG in Vglut2-Cre mice resulted in ipsilateral head-turning, while stimulation of the NRG in Vgat-Cre mice resulted in locomotion halt, due to body collapse probably related to spasms. Elicitation of locomotion could only be observed by stimulation of the LPGi in Vglut2-Cre mice (Capelli et al., 2017).

These results shift the interest in locomotion eliciting regions more towards the LPGi and away from the NRG. In line with the findings of previously mentioned studies as well as with the results of this study, the NRG's physiologic contribution to general locomotion is: (1) not essential, (2) mainly supportive through muscle tone regulation, (3) potentially involved in head stabilization and (4) functionally divided by its neural subpopulations.

Following research already focused on neuroanatomical and functional features of the LPGi, demonstrating its role in MLR-controlled context-specific locomotion, e.g. escape responses or explorative behavior (Caggiano et al., 2018). A loss-of-function experiment testing its essentiality in locomotion, analog to this experiment, has not yet been conducted. As for the NRG and other ReST nuclei, more research is needed in order to further untangle their diverse qualities in motor function. In this pursuit, it is important to continue choosing differentiated approaches, considering the functional differences in neural subpopulations. In addition to neurotransmitter-based approaches combined with precise definitions of regions of interest, as I used in this experiment, approaches targeting

---

cells identified by specific transcription features appear to be promising (Bouvier et al., 2015).

#### **5.4 Future strategies to investigate the ReST's potential for recovery from SCI**

This study investigated physiologic functions of the NRG in order to evaluate possible directions of further SCI research. Despite the NRG's non-essential role in general locomotion, it is not contradictory, that it still might hold great capacity for recovery. Neuroanatomical plasticity of the NRG has repeatedly been demonstrated, as well as its ability to contact long propriospinal interneurons, similar to the CST's ability to form detour circuits (Ballerman and Fouad, 2006; Filli et al., 2014, May et al., 2017).

In a pioneering work, that used chemogenetics in a contusion model in rats, significant functional recovery could, for the first time, be causally traced back to reticulospinal contributions (Asboth et al., 2018). It identified the ventral gigantocellular nucleus (vGi) as the major nucleus responsible for it and attributed the diverse distribution of the ReST in the white matter for its flexible plasticity, as it is highly probable, that spared fibers are to be found in any incomplete lesion.

Of particular interest is, that DREADD induced silencing of the vGi in intact mice did not have any behavioral effects, but the vGi still mediated recovery after SCI (Asboth et al., 2018). This led me to the following conclusions: (1) the NRG might significantly contribute to recovery, if it is spared and (2) multiple nuclei or subpopulations of the ReST might possess anatomical and functional regenerative capacities, depending on the injury pattern. Possibly the vGi mediated recovery, because it was the nucleus with the most spared fibers, meaning in different injury patterns with a different set of spared fibers, other nuclei may instead mediate it.

In conclusion, while it is now evident, that the ReST plays a key role in recovery after SCI, it remains elusive, which of its nuclei and tracts holds the highest potential for recovery, or if there are any substantial differences at all. Together with recent advances in physiologic locomotion research mentioned above, the investigation of the LPGi in SCI models appears to be of major interest. Additionally, the distribution of fibers of neural subpopulations of the different nuclei of the ReST in intact mice and in SCI models

---

requires a revising examination, as previous experiments often referred to them with insufficient precision.

---

## 6 References

- Adams, M. M., & Hicks, A. L. (2005). Spasticity after Spinal Cord Injury. *Spinal Cord*, 43, 577–586.
- Ahuja, C. S., Martin, A. R., & Fehlings, M. (2016). Recent Advances in Managing a Spinal Cord Injury Secondary to Trauma. *F1000Research*, 5.
- Ahuja, C. S., Wilson, J. R., Nori, S., Kotter, M. R. N., Druschel, C., Curt, A., & Fehlings, M. G. (2017). Traumatic Spinal Cord Injury. *Nature Reviews. Disease Primers*, 3, 17018.
- Babicki, S., Arndt, D., Marcu, A., Liang, Y., Grant, J. R., Maciejewski, A., & Wishart, D. S. (2016). Heatmapper: Web-Enabled Heat Mapping for All. *Nucleic Acids Research*, 44, W147-153.
- Ballermann, M., & Fouad, K. (2006). Spontaneous Locomotor Recovery in Spinal Cord Injured Rats Is Accompanied by Anatomical Plasticity of Reticulospinal Fibers. *European Journal of Neuroscience*, 23, 1988–1996.
- Bareyre, F. M., Kerschensteiner, M., Raineteau, O., Mettenleiter, T. C., Weinmann, O., & Schwab, M. E. (2004). The injured spinal cord spontaneously forms a new intraspinal circuit in adult rats. *Nature Neuroscience*, 7, 269–277.
- Bareyre, F. M., Kerschensteiner, M., Misgeld, T., & Sanes, J. R. (2005). Transgenic Labeling of the Corticospinal Tract for Monitoring Axonal Responses to Spinal Cord Injury. *Nature Medicine*, 11, 1355–1360.
- Batchelor, P. E., Wills, T. E., Skeers, P., Battistuzzo, C. R., Macleod, M. R., Howells, D. W., & Sena, E. S. (2013). Meta-Analysis of Pre-Clinical Studies of Early Decompression in Acute Spinal Cord Injury: A Battle of Time and Pressure. *PLOS ONE*, 8, e72659.
- Batka, R. J., Brown, T. J., Mcmillan, K. P., Meadows, R. M., Jones, K. J., & Haulcomb, M. M. (2014). The Need for Speed in Rodent Locomotion Analyses. *Anatomical record (Hoboken, N.J. : 2007)*, 297, 1839–1864.
- Bedbrook, C. N., Deverman, B. E., & Gradinaru, V. (2018). Viral Strategies for Targeting the Central and Peripheral Nervous Systems. *Annual Review of Neuroscience*, 41, 323–348.
- Blumenthal, M., Geng, V., Egen, C., & Gutenbrunner, C. (2017). People with Spinal Cord Injury in Germany. *American Journal of Physical Medicine & Rehabilitation*, 96, S66–S70.
- Bouvier, J., Caggiano, V., Leiras, R., Caldeira, V., Bellardita, C., Balueva, K., Kiehn, O. (2015). Descending Command Neurons in the Brainstem That Halt Locomotion. *Cell*, 163, 1191–1203.
- Bracken, M. B., & Holford, T. R. (1993). Effects of Timing of Methylprednisolone or Naloxone Administration on Recovery of Segmental and Long-Tract Neurological Function in NASCIS 2. *Journal of Neurosurgery*, 79, 500–507.
- Bracken, M. B., Shepard, M. J., Holford, T. R., Leo-Summers, L., Aldrich, E. F., Fazl, M., ... Young, W. (1997). Administration of Methylprednisolone for 24 or 48 Hours or Tirilazad Mesylate for 48 Hours in the Treatment of Acute Spinal Cord Injury. Results of the Third National Acute Spinal Cord Injury Randomized Controlled Trial. *National Acute Spinal Cord Injury Study. JAMA*, 277, 1597–1604.
- Bradley, P. M., Denecke, C. K., Aljovic, A., Schmalz, A., Kerschensteiner, M., & Bareyre, F. M. (2019). Corticospinal Circuit Remodeling after Central Nervous System Injury Is Dependent on Neuronal Activity. *Journal of Experimental Medicine*, 216, 2503–2514.

- 
- Brand, R. van den, Heutschi, J., Barraud, Q., DiGiovanna, J., Bartholdi, K., Huerlimann, M., Courtine, G. (2012). Restoring Voluntary Control of Locomotion after Paralyzing Spinal Cord Injury. *Science*, 336, 1182–1185.
- Braughler, J. M., & Hall, E. D. (1984). Effects of Multi-Dose Methylprednisolone Sodium Succinate Administration on Injured Cat Spinal Cord Neurofilament Degradation and Energy Metabolism. *Journal of Neurosurgery*, 61, 290–295.
- Bretzner, F., & Brownstone, R. M. (2013). Lhx3-Chx10 Reticulospinal Neurons in Locomotor Circuits. *Journal of Neuroscience*, 33, 14681–14692.
- Brown, A. R., & Martinez, M. (2018). Ipsilesional Motor Cortex Plasticity Participates in Spontaneous Hindlimb Recovery after Lateral Hemisection of the Thoracic Spinal Cord in the Rat. *The Journal of Neuroscience*, 38, 9977–9988.
- Brown, A. R., & Martinez, M. (2019). From Cortex to Cord: Motor Circuit Plasticity after Spinal Cord Injury. *Neural Regeneration Research*, 14, 2054–2062.
- Caballero-Garrido, E., Pena-Philippides, J. C., Galochkina, Z., Erhardt, E., & Roitbak, T. (2017). Characterization of Long-Term Gait Deficits in Mouse DMCAO, Using the CatWalk System. *Behavioural brain research*, 331, 282–296.
- Caggiano, V., Leiras, R., Goñi-Erro, H., Masini, D., Bellardita, C., Bouvier, J., Kiehn, O. (2018). Midbrain Circuits That Set Locomotor Speed and Gait Selection. *Nature*, 553, 455–460.
- Capelli, P., Pivetta, C., Esposito, M. S., & Arber, S. (2017). Locomotor Speed Control Circuits in the Caudal Brainstem. *Nature*, 551, 373–377.
- Cardenas, D. D., & Felix, E. R. (2009). Pain after Spinal Cord Injury: A Review of Classification, Treatment Approaches, and Treatment Assessment. *PM&R*, 1, 1077-1090.
- Chen, X., Choo, H., Huang, X.-P., Yang, X., Stone, O., Roth, B. L., & Jin, J. (2015). The First Structure–Activity Relationship Studies for Designer Receptors Exclusively Activated by Designer Drugs. *ACS Chemical Neuroscience*, 6, 476-484.
- Chen, Y., He, Y., & DeVivo, M. J. (2016). Changing Demographics and Injury Profile of New Traumatic Spinal Cord Injuries in the United States, 1972–2014. *Archives of Physical Medicine and Rehabilitation*, 97, 1610–1619.
- Courtine, G., Gerasimenko, Y., van den Brand, R., Yew, A., Musienko, P., Zhong, H., Edgerton, V. R. (2009). Transformation of Nonfunctional Spinal Circuits into Functional States after the Loss of Brain Input. *Nature Neuroscience*, 12, 1333–1342.
- Curt, A. (2012). Querschnittlähmung. In: Diener, H.-C., Weimar, C. (Eds) Leitlinien für Diagnostik und Therapie in der Neurologie. Stuttgart: Thieme Verlag.
- Dijkers, M. (1997). Quality of Life after Spinal Cord Injury: A Meta Analysis of the Effects of Disablement Components. *Spinal Cord*, 35, 829–840.
- Ditunno, J. F., Little, J. W., Tessler, A., & Burns, A. S. (2004). Spinal Shock Revisited: A Four-Phase Model. *Spinal Cord*, 42, 383–395.
- Donnelly, D. J., & Popovich, P. G. (2008). Inflammation and Its Role in Neuroprotection, Axonal Regeneration and Functional Recovery after Spinal Cord Injury. *Experimental neurology*, 209, 378–388.
- Du Beau, A., Shakya Shrestha, S., Bannatyne, B. A., Jaliczy, S. M., Linnen, S., & Maxwell, D. J. (2012). Neurotransmitter Phenotypes of Descending Systems in the Rat Lumbar Spinal Cord. *Neuroscience*, 227, 67–79.
- Dumont, R. J., Okonkwo, D. O., Verma, S., Hurlbert, R. J., Boulos, P. T., Ellegala, D. B., & Dumont, A. S. (2001). Acute Spinal Cord Injury, Part I: Pathophysiologic Mechanisms. *Clinical Neuropharmacology*, 24, 254–264.

- 
- Exner, G. Der Arbeitskreis „Querschnittlähmungen“ des Hauptverbandes der gewerblichen Berufsgenossenschaften in Deutschland Fakten-Zahlen-Prognosen. Trauma und Berufskrankheit, 2.
- Fehlings, M. G., Tetreault, L. A., Wilson, J. R., Kwon, B. K., Burns, A. S., Martin, A. R., Harrop, J. S. (2017). A Clinical Practice Guideline for the Management of Acute Spinal Cord Injury: Introduction, Rationale, and Scope. *Global Spine Journal*, 7, 84S-94S.
- Fehlings, M. G., & Perrin, R. G. (2006). The Timing of Surgical Intervention in the Treatment of Spinal Cord Injury: A Systematic Review of Recent Clinical Evidence. *Spine*, 31, S28.
- Fehlings, M. G., Vaccaro, A., Wilson, J. R., Singh, A., W Cadotte, D., Harrop, J. S., Rampersaud, R. (2012). Early versus Delayed Decompression for Traumatic Cervical Spinal Cord Injury: Results of the Surgical Timing in Acute Spinal Cord Injury Study (STASCIS). *PloS One*, 7, e32037.
- Felten, D., O’Banion, M., Maida, M. (2015). *Netter’s Atlas of Neuroscience*. 3rd Edition. Amsterdam: Elsevier.
- Fiander, M. D. J., Stifani, N., Nichols, M., Akay, T., & Robertson, G. S. (2017). Kinematic Gait Parameters Are Highly Sensitive Measures of Motor Deficits and Spinal Cord Injury in Mice Subjected to Experimental Autoimmune Encephalomyelitis. *Behavioural Brain Research*, 317, 95–108.
- Filli, L., Engmann, A. K., Zörner, B., Weinmann, O., Moraitis, T., Gullo, M., ... Schwab, M. E. (2014). Bridging the Gap: A Reticulo-Propriospinal Detour Bypassing an Incomplete Spinal Cord Injury. *Journal of Neuroscience*, 34, 13399–13410.
- Gabriel, A. F., Marcus, M. A. E., Honig, W. M. M., Walenkamp, G. H. I. M., & Joosten, E. A. J. (2007). The CatWalk Method: A Detailed Analysis of Behavioral Changes after Acute Inflammatory Pain in the Rat. *Journal of Neuroscience Methods*, 163, 9–16.
- Galeiras Vázquez, R., Ferreiro Velasco, M. E., Mourelo Fariña, M., Montoto Marqués, A., & Salvador de la Barrera, S. (2017). Update on Traumatic Acute Spinal Cord Injury. Part 1. *Medicina Intensiva (English Edition)*, 41, 237–247.
- Gomez, J. L., Bonaventura, J., Lesniak, W., Mathews, W. B., Syta-Shah, P., Rodriguez, L. A., ... Michaelides, M. (2017). Chemogenetics Revealed: DREADD Occupancy and Activation via Converted Clozapine. *Science*, 357, 503–507.
- Guly, H. R., Bouamra, O., & Lecky, F. (2008). The Incidence of Neurogenic Shock in Patients with Isolated Spinal Cord Injury in the Emergency Department. *Resuscitation*, 76, 57–62.
- Häggglund, M., Borgius, L., Dougherty, K. J., & Kiehn, O. (2010). Activation of Groups of Excitatory Neurons in the Mammalian Spinal Cord or Hindbrain Evokes Locomotion. *Nature Neuroscience*, 13, 246–252.
- Hall, E. D., & Braughler, J. M. (1982). Effects of Intravenous Methylprednisolone on Spinal Cord Lipid Peroxidation and (Na<sup>+</sup> + K<sup>+</sup>)-ATPase Activity: Dose-Response Analysis during 1st Hour after Contusion Injury in the Cat. *Journal of Neurosurgery*, 57, 247–253.
- Hamers, F. P. T., Koopmans, G. C., & Joosten, E. A. J. (2006). CatWalk-Assisted Gait Analysis in the Assessment of Spinal Cord Injury. *Journal of Neurotrauma*, 23, 537–548.
- Hamm, R., Pike, B., O’Dell, D., Lyeth, B., & Jenkins, L. (1994). The Rotarod Test: An Evaluation of Its Effectiveness in Assessing Motor Deficits Following Traumatic Brain Injury. *Journal of Neurotrauma*, 11, 187–196.

- 
- Honeycutt, C. F., Kharouta, M., & Perreault, E. J. (2013). Evidence for Reticulospinal Contributions to Coordinated Finger Movements in Humans. *Journal of Neurophysiology*, 110, 1476–1483.
- Ilg, A.-K., Enkel, T., Bartsch, D., & Böhner, F. (2018). Behavioral Effects of Acute Systemic Low-Dose Clozapine in Wild-Type Rats: Implications for the Use of DREADDs in Behavioral Neuroscience. *Frontiers in Behavioral Neuroscience*, 12.
- Jacobi, A., Loy, K., Schmalz, A. M., Hellsten, M., Umemori, H., Kerschensteiner, M., & Bareyre, F. M. (2015). FGF22 Signaling Regulates Synapse Formation during Post-Injury Remodeling of the Spinal Cord. *The EMBO Journal*, 34, 1231–1243.
- Jendryka, M., Palchadhuri, M., Ursu, D., Veen, B. van der, Liss, B., Kätzel, D., Pekcec, A. (2019). Pharmacokinetic and Pharmacodynamic Actions of Clozapine-N-Oxide, Clozapine, and Compound 21 in DREADD-Based Chemogenetics in Mice. *Scientific Reports*, 9, 1–14.
- Jordan, L. M. (1998). Initiation of Locomotion in Mammals. *Annals of the New York Academy of Sciences*, 860, 83–93.
- Kim, Y.-H., Ha, K.-Y., & Kim, S.-I. (2017). Spinal Cord Injury and Related Clinical Trials. *Clinics in Orthopedic Surgery*, 9, 1–9.
- Kirshblum, S. C., Waring, W., Biering-Sorensen, F., Burns, S. P., Johansen, M., Schmidt-Read, M., ... Krassioukov, A. (2011). Reference for the 2011 Revision of the International Standards for Neurological Classification of Spinal Cord Injury. *The Journal of Spinal Cord Medicine*, 34, 547–554.
- Klusman, I., & Schwab, M. E. (1997). Effects of Pro-Inflammatory Cytokines in Experimental Spinal Cord Injury. *Brain Research*, 762, 173–184.
- Koopmans, G. C., Deumens, R., Honig, W. M. M., Hamers, F. P. T., Steinbusch, H. W. M., & Joosten, E. A. J. (2005). The Assessment of Locomotor Function in Spinal Cord Injured Rats: The Importance of Objective Analysis of Coordination. *Journal of Neurotrauma*, 22, 214–225.
- Krashes, M. J., Koda, S., Ye, C., Rogan, S. C., Adams, A. C., Cusher, D. S., Lowell, B. B. (2011). Rapid, Reversible Activation of AgRP Neurons Drives Feeding Behavior in Mice. *The Journal of Clinical Investigation*, 121, 1424–1428.
- La Rosa, G., Conti, A., Cardali, S., Cacciola, F., & Tomasello, F. (2004). Does Early Decompression Improve Neurological Outcome of Spinal Cord Injured Patients? Appraisal of the Literature Using a Meta-Analytical Approach. *Spinal Cord*, 42, 503–512.
- Lammertse, D., Dungan, D., Dreisbach, J., Falci, S., Flanders, A., Marino, R., & Schwartz, E. (2007). Neuroimaging in Traumatic Spinal Cord Injury: An Evidence-Based Review for Clinical Practice and Research. *The Journal of Spinal Cord Medicine*, 30, 205–214.
- Lemieux, M., & Bretzner, F. (2019). Glutamatergic Neurons of the Gigantocellular Reticular Nucleus Shape Locomotor Pattern and Rhythm in the Freely Behaving Mouse. *PLOS Biology*, 17, e2003880.
- Lendemanns, S., & Ruchholtz, S. (2012). S3-Leitlinie Polytrauma/Schwerverletzten-Behandlung. *Der Unfallchirurg*, 115, 14–21.
- Liebscher, T., Schnell, L., Schnell, D., Scholl, J., Schneider, R., Gullo, M., Schwab, M. E. (2005). Nogo-A antibody improves regeneration and locomotion of spinal cord-injured rats. *Annals of Neurology*, 58, 706–719.
- Liu, D., Xu, G.-Y., Pan, E., & McAdoo, D. J. (1999a). Neurotoxicity of Glutamate at the Concentration Released upon Spinal Cord Injury. *Neuroscience*, 93, 1383–1389.

- 
- Liu, D., Xu, G. Y., Pan, E., & McAdoo, D. J. (1999b). Neurotoxicity of Glutamate at the Concentration Released upon Spinal Cord Injury. *Neuroscience*, 93, 1383–1389.
- Loy, K., Schmalz, A., Hoche, T., Jacobi, A., Kreutzfeldt, M., Merkler, D., & Bareyre, F. M. (2018). Enhanced Voluntary Exercise Improves Functional Recovery Following Spinal Cord Injury by Impacting the Local Neuroglial Injury Response and Supporting the Rewiring of Supraspinal Circuits. *Journal of Neurotrauma*, 35, 2904–2915.
- Mahler, S. V., Vazey, E. M., Beckley, J. T., Keistler, C. R., McGlinchey, E. M., Kaufling, J., ... Aston-Jones, G. (2014). Designer Receptors Show Role for Ventral Pallidum Input to Ventral Tegmental Area in Cocaine Seeking. *Nature Neuroscience*, 17, 577–585.
- Mahler, S. V., & Aston-Jones, G. (2018). CNO Evil? Considerations for the Use of DREADDs in Behavioral Neuroscience. *Neuropsychopharmacology*, 43, 934–936.
- Manohar, A., Foffani, G., Ganzer, P. D., Bethea, J. R., & Moxon, K. A. Cortex-Dependent Recovery of Unassisted Hindlimb Locomotion after Complete Spinal Cord Injury in Adult Rats. *eLife*, 6.
- Manvich, D. F., Webster, K. A., Foster, S. L., Farrell, M. S., Ritchie, J. C., Porter, J. H., & Weinshenker, D. (2018). The DREADD Agonist Clozapine N -Oxide (CNO) Is Reverse-Metabolized to Clozapine and Produces Clozapine-like Interoceptive Stimulus Effects in Rats and Mice. *Scientific Reports*, 8, 3840.
- Marino, R. J., Jones, L., Kirshblum, S., Tal, J., & Dasgupta, A. (2008). Reliability and Repeatability of the Motor and Sensory Examination of the International Standards for Neurological Classification of Spinal Cord Injury. *The Journal of Spinal Cord Medicine*, 31, 166–170.
- Markham, C. H. (1987). Vestibular Control of Muscular Tone and Posture. *The Canadian Journal of Neurological Sciences. Le Journal Canadien Des Sciences Neurologiques*, 14, 493–496.
- May, Z., Fenrich, K. K., Dahlby, J., Batty, N. J., Torres-Espín, A., & Fouad, K. (2017). Following Spinal Cord Injury Transected Reticulospinal Tract Axons Develop New Collateral Inputs to Spinal Interneurons in Parallel with Locomotor Recovery. *Neural Plasticity*, 2017.
- McCall, A. A., Miller, D. M., & Yates, B. J. (2017). Descending Influences on Vestibulospinal and Vestibulosympathetic Reflexes. *Frontiers in Neurology*, 8.
- McDonald, J. W., Liu, X.-Z., Qu, Y., Liu, S., Mickey, S. K., Turetsky, D., Choi, D. W. (1999). Transplanted Embryonic Stem Cells Survive, Differentiate and Promote Recovery in Injured Rat Spinal Cord. *Nature Medicine*, 5, 1410–1412.
- van Meeteren, N. L. U., Eggers, R., Lankhorst, A. J., Gispén, W. H., & Hamers, F. P. T. (2003). Locomotor Recovery after Spinal Cord Contusion Injury in Rats Is Improved by Spontaneous Exercise. *Journal of Neurotrauma*, 20, 1029–1037.
- Metsalu, T., & Vilo, J. (2015). ClustVis: A Web Tool for Visualizing Clustering of Multivariate Data Using Principal Component Analysis and Heatmap. *Nucleic Acids Research*, 43, W566–W570.
- Metz, G. A., & Whishaw, I. Q. (2009). The Ladder Rung Walking Task: A Scoring System and Its Practical Application. *Journal of Visualized Experiments: JoVE*.
- Nathan, P. W., Smith, M., & Deacon, P. (1996). Vestibulospinal, Reticulospinal and Descending Propriospinal Nerve Fibres in Man. *Brain: A Journal of Neurology*, 119 (Pt 6), 1809–1833.

- 
- National Spinal Cord Injury Statistical Center, Birmingham, Alabama. (2012). Spinal Cord Injury Facts and Figures at a Glance. *The Journal of Spinal Cord Medicine*, 35, 197-198.
- Noga, B. R., Kriellaars, D. J., Brownstone, R. M., & Jordan, L. M. (2003). Mechanism for Activation of Locomotor Centers in the Spinal Cord by Stimulation of the Mesencephalic Locomotor Region. *Journal of Neurophysiology*, 90, 1464–1478.
- O’Shea, T. M., Burda, J. E., & Sofroniew, M. V. Cell Biology of Spinal Cord Injury and Repair. *The Journal of Clinical Investigation*, 127, 3259–3270.
- Oyinbo, C. A. (2011). Secondary Injury Mechanisms in Traumatic Spinal Cord Injury: A Nugget of This Multiply Cascade. *Acta Neurobiologiae Experimentalis*, 71, 281–299.
- Paxinos, G., Franklin, K. (2019). Paxinos and Franklin's the Mouse Brain in Stereotaxic Coordinates. 5<sup>th</sup> Edition. Cambridge: Academic Print. Paxinos, G., Franklin, K. (2019). Paxinos and Franklin's the Mouse Brain in Stereotaxic Coordinates. 5<sup>th</sup> Edition. Cambridge: Academic Print.
- Petrosyan, H. A., Hunanyan, A. S., Alessi, V., Schnell, L., Levine, J., & Arvanian, V. L. (2013). Neutralization of Inhibitory Molecule NG2 Improves Synaptic Transmission, Retrograde Transport, and Locomotor Function after Spinal Cord Injury in Adult Rats. *Journal of Neuroscience*, 33, 4032–4043.
- Ray, S. K., Hogan, E. L., & Banik, N. L. (2003). Calpain in the Pathophysiology of Spinal Cord Injury: Neuroprotection with Calpain Inhibitors. *Brain Research. Brain Research Reviews*, 42, 169–185.
- Riddle, C. N., Edgley, S. A., & Baker, S. N. (2009). Direct and Indirect Connections with Upper Limb Motoneurons from the Primate Reticulospinal Tract. *The Journal of Neuroscience*, 29, 4993–4999.
- Roth, B. L. (2016). DREADDs for Neuroscientists. *Neuron*, 89, 683–694.
- Sangari, S., & Perez, M. A. (2019). Imbalanced Corticospinal and Reticulospinal Contributions to Spasticity in Humans with Spinal Cord Injury. *Journal of Neuroscience*, 39, 7872–7881.
- Sekhon, L. H. S., & Fehlings, M. G. (2001). Epidemiology, Demographics, and Pathophysiology of Acute Spinal Cord Injury. *Spine*, 26, S2.
- Siegel, C. S., Fink, K. L., Strittmatter, S. M., & Cafferty, W. B. J. (2015). Plasticity of Intact Rubral Projections Mediates Spontaneous Recovery of Function after Corticospinal Tract Injury. *Journal of Neuroscience*, 35, 1443–1457.
- Singh, A., Tetreault, L., Kalsi-Ryan, S., Nouri, A., & Fehlings, M. G. (2014). Global Prevalence and Incidence of Traumatic Spinal Cord Injury. *Clinical Epidemiology*, 6, 309–331.
- Silva, N. A., Sousa, N., Reis, R. L., & Salgado, A. J. (2014). From Basics to Clinical: A Comprehensive Review on Spinal Cord Injury. *Progress in Neurobiology*, 114, 25–57.
- Smith, K. S., Bucci, D. J., Luikart, B. W., & Mahler, S. V. (2016). DREADDs: Use and Application in Behavioral Neuroscience. *Behavioral Neuroscience*, 130, 137–155.
- Sofroniew, M. V. (2018). Dissecting Spinal Cord Regeneration. *Nature*, 557, 343–350.
- Soteropoulos, D. S., Williams, E. R., & Baker, S. N. (2012). Cells in the Monkey Ponto-Medullary Reticular Formation Modulate Their Activity with Slow Finger Movements. *The Journal of Physiology*, 590, 4011–4027.
- Stroobants, S., Gantois, I., Pooters, T., & D’Hooge, R. (2013). Increased Gait Variability in Mice with Small Cerebellar Cortex Lesions and Normal Rotarod Performance. *Behavioural Brain Research*, 241, 32–37.
- Takakusaki, K., Chiba, R., Nozu, T., & Okumura, T. (2016). Brainstem Control of Locomotion and Muscle Tone with Special Reference to the Role of the

- 
- Mesopontine Tegmentum and Medullary Reticulospinal Systems. *Journal of Neural Transmission*, 123, 695–729.
- Vaccaro, A. R., Oner, C., Kepler, C. K., Dvorak, M., Schnake, K., Bellabarba, C., AOSpine Spinal Cord Injury & Trauma Knowledge Forum. (2013). AOSpine Thoracolumbar Spine Injury Classification System: Fracture Description, Neurological Status, and Key Modifiers. *Spine*, 38, 2028–2037.
- Vaccaro, A. R., Koerner, J. D., Radcliff, K. E., Oner, F. C., Reinhold, M., Schnake, K. J., Vialle, L. R. (2016). AOSpine Subaxial Cervical Spine Injury Classification System. *European Spine Journal: Official Publication of the European Spine Society, the European Spinal Deformity Society, and the European Section of the Cervical Spine Research Society*, 25, 2173–2184.
- Vadhan, J., & M Das, J. (2020). Neuroanatomy, Red Nucleus. In *StatPearls p. Treasure Island (FL): StatPearls Publishing*.
- Vrinten, D. H., & Hamers, F. F. T. (2003). ‘CatWalk’ Automated Quantitative Gait Analysis as a Novel Method to Assess Mechanical Allodynia in the Rat; a Comparison with von Frey Testing. *Pain*, 102, 203–209.
- Wang, D. (2009). Reticular Formation and Spinal Cord Injury. *Spinal Cord*, 47, 204–212.
- Weidner, N., Ner, A., Salimi, N., & Tuszynski, M. H. (2001). Spontaneous Corticospinal Axonal Plasticity and Functional Recovery after Adult Central Nervous System Injury. *Proceedings of the National Academy of Sciences of the United States of America*, 98, 3513–3518.
- Whishaw, I. Q., Gorny, B., & Sarna, J. (1998). Paw and Limb Use in Skilled and Spontaneous Reaching after Pyramidal Tract, Red Nucleus and Combined Lesions in the Rat: Behavioral and Anatomical Dissociations. *Behavioural Brain Research*, 93, 167–183.
- Zerbi, V., Floriou-Servou, A., Markicevic, M., Vermeiren, Y., Sturman, O., Privitera, M., Bohacek, J. (2019). Rapid Reconfiguration of the Functional Connectome after Chemogenetic Locus Coeruleus Activation. *Neuron*, 103, 702-718.e5.
- Zhou, W., Cheung, K., Kyu, S., Wang, L., Guan, Z., Kurien, P. A., ... Jan, L. Y. (2018). Activation of Orexin System Facilitates Anesthesia Emergence and Pain Control. *Proceedings of the National Academy of Sciences of the United States of America*, 115, E10740–E10747.
- Zörner, B., Filli, L., Starkey, M. L., Gonzenbach, R., Kasper, H., Röthlisberger, M., Schwab, M. E. (2010). Profiling Locomotor Recovery: Comprehensive Quantification of Impairments after CNS Damage in Rodents. *Nature Methods*, 7, 701–708.

---

## **7 Acknowledgements**

First and foremost, I want to thank PD Dr. Florence Bareyre for granting me the great opportunity to do experiments in her lab and for the outstanding supervision of my thesis. Her scientific advice, dedication and openness never fell short. I learned a lot during this time and left with a sparking interest in neuroscience.

Next, I want to thank my supervisor and longtime friend Dr. Carmen Denecke for the suggestion of the project, the effort she put into it, her team spirit and her lively humor.

Thanks to my colleagues in the lab for all the friendly assistance and advice, which I received on countless accounts. In particular, I want to thank Almir Aljovic and Laura Empel for the time we shared in and outside of the lab.

Of course, I am very grateful for all the support from my parents, through my long years of studying. Special thanks go to my father for his scientific advice.

Lastly, I want to thank Robin Rastetter for proofreading my thesis.

---

## Eidesstattliche Versicherung

**Pankratz, Benjamin Robert**

---

Name, Vorname

Ich erkläre hiermit an Eides statt,

dass ich die vorliegende Dissertation mit dem Thema

**Contribution of excitatory and inhibitory tract components of the reticulospinal tract to general locomotion**

selbstständig verfasst, mich außer der angegebenen keiner weiteren Hilfsmittel bedient und alle Erkenntnisse, die aus dem Schrifttum ganz oder annähernd übernommen sind, als solche kenntlich gemacht und nach ihrer Herkunft unter Bezeichnung der Fundstelle einzeln nachgewiesen habe.

Ich erkläre des Weiteren, dass die hier vorgelegte Dissertation nicht in gleicher oder in ähnlicher Form bei einer anderen Stelle zur Erlangung eines akademischen Grades eingereicht wurde.

Freiburg, 14.08.2021

---

Ort, Datum

B. Pankratz

---

Unterschrift Doktorand